Geological Survey of Finland

Bulletin 299

Structure, mineralogy and chemistry of the Syöte section in the Early Proterozoic Koillismaa layered intrusion, northeastern Finland

by Tuomo Alapieti, Rauno Hugg
and Tauno Piirainen

Geologinen tutkimuslaitos · Espoo 1979

Geologial Survey of Finland, Bulletin 299

STRUCTURE, MINERALOGY AND CHEMISTRY OF THE SYÖTE SECTION IN THE EARLY PROTEROZOIC KOILLISMAA LAYERED INTRUSION, NORTHEASTERN FINLAND

by

TUOMO ALAPIETI, RAUNO HUGG and TAUNO PIIRAINEN

with 18 figures and 12 tables in the text

GEOLOGINEN TUTKIMUSLAITOS
ESPOO 1979

Alapieti, T., Hugg, R. & Piirainen, T. 1979. Structure, mineralogy and chemistry of the Syöte section in the Early Proterozoic Koillismaa layered intrusion, northeastern Finland. *Geological Survey of Finland, Bulletin 299.* 43 pages, 18 figures, and 12 tables.

The Syöte formation represents a section of the K o i l l i s m a a layered intrusion, which was formed in the Early Proterozoic era between an Archaean basement and Proterozoic volcanics. The section may be divided into a relatively thin marginal series and a layered series some 3 km thick, characterized by rhythmic and cryptic layering. The lower zone of the layered series is composed of plagioclase-olivine-orthopyroxene mesocumulates and/or adcumulates containing Ca-rich clinopyroxene and iron-titanium oxides as intercumulus grains. The rocks of the middle zone are plagioclase-inverted pigeonite-augite orthocumulates and/or mesocumulates, while in the upper zone very much larger amounts of plagioclase are found, and the dominant rocks are gabbroic anorthosites and anorthositic gabbros. A magnetite gabbro horizon occurs in the lower part of this zone.

The differentiation curves tend to be short, and especially those for the lower zone, uneven. The crystallization index varies between 69.02 and 49.35. Equilibration temperatures determined after Wood & Banno give values of approx. 1000°C for the rocks in the lower part of the intrusion and 870°C for the upper part.

Authors' addresses:

Tuomo Alapieti and Tauno Piirainen, Department of Geology, University of Oulu, SF-90100 Oulu 10, Finland.
Rauno Hugg, Rautaruukki Co., SF-90100 Oulu 10, Finland.

ISBN 951-690-100-x
ISSN 0367-522x

Helsinki 1979. Valtion painatuskeskus

CONTENTS

INTRODUCTION

The Syöte, Porttivaara and Kuusijärvi areas of *Koillismaa*, or northeastern Finland (Fig. 1), possess extensive occurrences of basic ignenous rocks which have been termed 'Syöte-type gabbros' (Enkovaara *et al.* 1953, Väyrynen 1954). In order to determine the mode of occurrence, composition and ore deposits of these, the Koillismaa Research Project was set up at the University of Oulu in 1971—76, the findings of which suggest that Syöte, Porttivaara and Kuusijärvi are not separate intrusions but sections of the same intrusion which have moved apart one from another (Piirainen *et al.* 1978). At the same time, a strong, narrow positive gravity anomaly extends from the Porttivaara-Kuusijärvi blocks to the ultramafic massif of Näränkävaara on the border with the Soviet Union, indicating that the Näränkävaara massif and the Syöte-type gabbros belong to the production of the same igneous activity. All these blocks posses structural features typical of layered intrusions, rhythmic and cryptic layering and igneous lamination. The age of the rocks is the same at Näränkävaara and Porttivaara, 2440 Ma (Kouvo, personal communication), and they together constitute an entity which resembles known examples of layered intrusions. This entity will be referred to here as the Koillismaa layered igneous intrusion. Näränkävaara represents the deepest part of this intrusion, in which a thick sequence of ferromagnesian silicate cumulates is visible in a feeder channel intersecting Archaean granitoids (Alapieti *et al.* 1979). The Porttivaara, Kuusijärvi and Syöte sections located some 60—80 km further west then represent the upper horizons.

Research already carried out on the Porttivaara section provides a description of its structure and composition and examines solutions to various questions concerning its petrology and metallogenetic properties (Piirainen & Juopperi 1968, Mäkelä 1975, Juopperi 1977, Piirainen *et al.* 1977). Interest in this block has been further stimulated by the discovery of vanadium ore at Mustavaara and sulphide-bearing disseminations in the marginal zone of the section. In contrast, little is known about Syöte itself, even though the basic rock types characteristic of the whole area were previously named after it. Extensive material has been assembled on this section in the course of the Koillismaa project, but it has not yet been possible to analyse or evaluate this. The present paper thus aims to provide, on the basis of this material, a general description of the section and a framework within which to examine the relations between basic magma crystallization and ore forming processes in the Koillismaa intrusion as a whole.

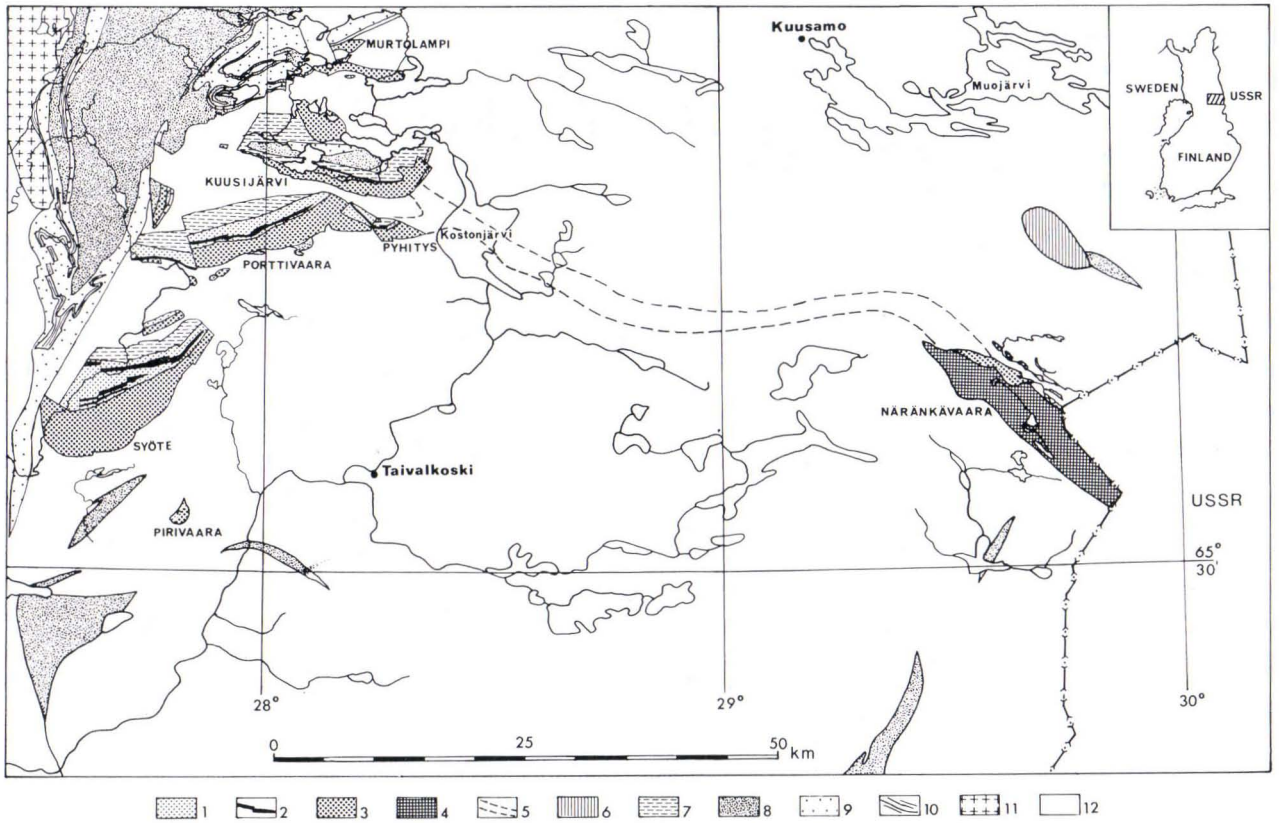

Fig. 1. Simplified geological map of the Koillismaa layered intrusion with immediate surroundings.

Koillismaa layered intrusion

1. Leucogabbro & Anorthosite
2. Magnetite gabbro
3. Norite & Gabbronorite
4. Ultramafic rocks
5. Connecting 'dyke'
6. Alkaline rock (post-Gambrian)

Surroundings

7. Biotite-albite rock
8. Greenstone & Amphibolite
9. Quartzite
10. Mica schist
11. Granite
12. Basement granite gneiss.

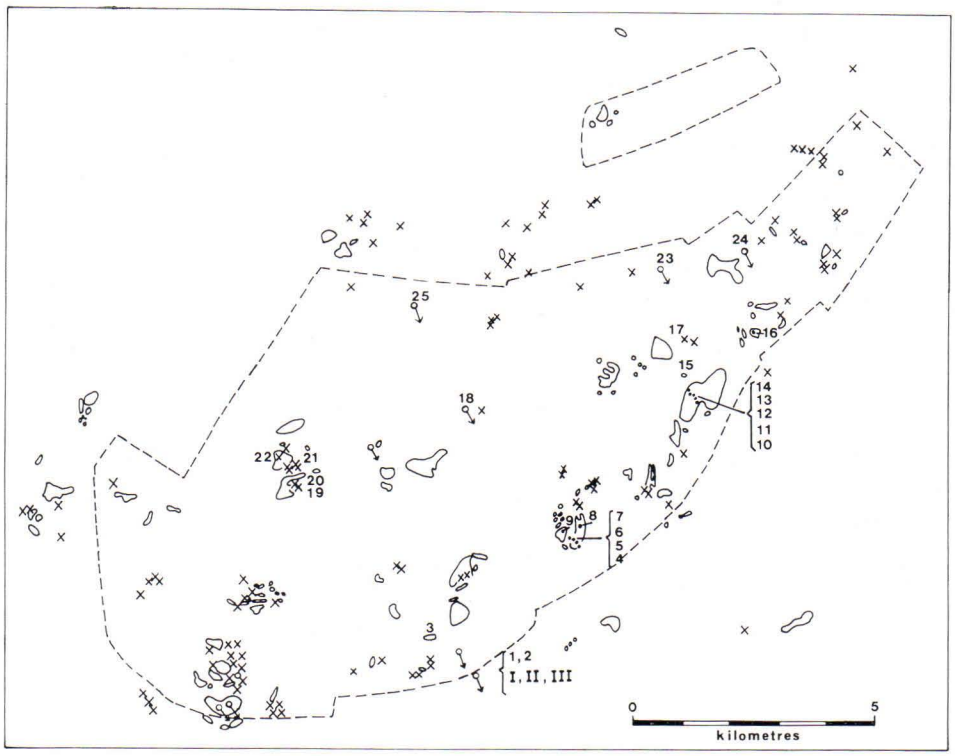

Fig. 2. Simplified map of the Syöte area (see Fig. 3.) indicating type sample sites and the distribution of the outcrops. Cross = small outcrop; solid circle = extensive outcrop.

A sample of 28 specimens was selected from the material gathered in connection with the Koillismaa Project (Table 1, Fig. 2) to be subjected to detailed laboratory analysis, an attempt being made to select these in such a way as to be maximally representative of the whole area of the section from bottom to top. A second quiding principle was that each specimen should contain as many primary minerals as possible, as an aid to the recognition of cryptic layering. As a result of the alteration in the rocks, it proved especially difficult in many areas to find any primary ferromagnesian silicates.

The whole-rock analyses from these type samples were carried out at the Research Laboratory of the Raahe Steel Works of Rautaruukki Co., mainly using XRF techniques. Ferrous iron content was determined titrimetrically at the Geochemical Laboratory of the Department of Geology, University of Oulu.

The mineral analyses were carried out at the Institute of Electron Optics, University of Oulu, using a JEOL JXA — 3SM electron microprobe. The conditions for quantitative analysis were: 15 kV accelerating voltage and approximately 0.05 μA specimen current (measured on metallic Cu) for Si, Ti, Al, Fe, Mg, Ca, Na and

Table 1.

Type samples for the Syöte section and their modal classification.

Layered series		
1*	B10/107.55 m**	Olivine gabbronorite
2	B10/33.65 m	Olivine gabbro
3	HK-6	Olivine gabbronorite
4	K0061A-1	Leuco-olivine gabbronorite
5	K0061A-3	Leucogabbro
6	K0061C	Olivine gabbronorite
7	K0062B-2	Olivine gabbronorite
8	K0067B-2	Leuconorite
9	K0063B	Olivine norite
10	K0189	Leucogabbronorite
11	K0190	Leucogabbro
12	K0191	Gabbronorite
13	K0192	Gabbronorite
14	K0193	Leucogabbronorite
15	K0106	Gabbro
16	K0112	Leucogabbronorite
17	K0209	Gabbronorite
18	B9/114.6 m	Quartz anorthosite
19	K0051B	Gabbro (Magnetite-bearing)
20	K0050A	Magnetite gabbro
21	K0044F	Magnetite gabbro
22	K0042D	Gabbro (Magnetite-bearing)
23	SR2/55 m	Magnetite gabbro
24	SR3/132 m	Magnetite gabbro
25	B11/39.45 m	Quartz anorthosite
Marginal series		
I	B10/164,6 m	Metaperidotite
II	B10/168.8 m	Contact gabbro
III	B10/249,55 m	Contact gabbro

* Numbering used in the text and tables.
** Serial numbers in the Koillismaa Research Project.

K, and 25 kV accelerating voltage and approximately 0.3 μA specimen current for the remaining elements. The following standards were used: quartz for Si, TiO for Ti, synthetic sapphire for Al, hematite for Fe, periclase for Mg, wollastonite for Ca, albite for Na, sanidine for K and metallic Mn and Cr. The ZAF corrections were processed using the MKl computer program of Mason *et al.* (1969), and the plagioclase analyses were performed using the 'feldspar' method of the same authors, in which only Ca, Na, K (and Fe) in the plagioclase were measured and the program calculated the remaining elements for correction purposes, on the assumption that the minerals are stoichiometric. In augites and inverted pigeonites showing the coarse type of exsolution lamellae only the host phase was analysed, using a beam focussed to a diameter of approximately 2 μm. This procedure certainly exaggerates the Ca content in augites and underestimates it in inverted pigeonites. In the iron-titanium oxides, when it was not possible to obtain individual analyses for the host oxide and exolution lamellae, the beam was defocussed ($\sim$20 μm) and the bulk composition of the two phases thus obtained.

STRUCTURE AND PETROGRAPHY OF THE SYÖTE SECTION

The Syöte section was surveyed geologically as part of the work of the Koillismaa project, employing magnetic and gravimetric measurements. The geological map resulting from this investigation is presented in Fig. 3. As may be seen from the map, the section is 20 km in length in a SW—NE direction, and reaches a maximum breadth of 10 km. An interpretation of certain geophysical measurements (Ruotsalainen 1977) suggests that the maximum depth of the present under-surface of the section is no more than 1.1 km. Structural features typical of layered intrusions, i.e. rhythmic layering and igneous lamination, are well in evidence in places, and these are oriented broadly in the same direction as the longitudinal axis of the section itself i.e. SW—NE, with a dip of 30°—40° to the NW. The original thickness of the whole sequence is estimated to be about 3 km, and since the section is cut by a number of faults, repetitions are to be found in the layering, as may be seen in the map.

The foot wall of the section borders on a broad expanse of Archaean granitoids some 2 700—2 800 Ma in age, which became altered at the contact with the intrusion due to the heating effect of the basic magma to form an albite-quartz rock. The hanging wall of the intrusion is formed by biotite-albite rocks and greenstones which are clearly younger in age than the granitoids, and judging from their relict structure must be ancient keratophyric and basic volcanics respectively. No separate age determinations were carried out for the section, its age being assumed to be the same as that of Porttivaara and Näränkävaara, i.e. 2440 Ma (cf. p. 5).

Two parts may be distinquished within the section, a relatively thin marginal series and an extensive layered series. The marginal series borders on albite-quartz rock, which forms a breccia with the contact gabbros. These gabbros then grade upwards to ultramafic rocks, which are then followed by the rocks of the layered series itself, lying at an oblique angle to the marginal series. Typical rocks of the lower part of the layered series are olivine gabbronorites and gabbronorites, while the upper part is characterized by leucogabbros and anorthosites. A clearly-defined horizon of magnetite gabbro is found in the lower part of the leucogabbro and anorthosite sequence.

The Syöte layered series may be divided into three zones, lower, middle and upper, on the basis of differences in mineral composition. The boundary between the lower and middle zones is the point at which olivine, a mineral typical of the lower zone, ceases to form as a cumulus mineral. The same boundary also marks a rise above the pigeonite-orthopyroxene inversion curve in the crystallization of Ca-poor pyroxene, so that the bronzite of the lower zone now gives way to pigeonite, while Ca-rich pyroxene begins to crystallize as a cumulus mineral.

The boundary between the middle and upper zones is not quite so clearly marked, although above it the amounts of plagioclase definitely exceed those of the mafic minerals, whereas in the middle zone various norites are dominant. This boundary

Fig. 3. Geological map of the Syöte area.

Fig. 4. Layering in the lower zone.

is nevertheless very easy to distinguish in the field, whereas that between the lower and middle zones presents greater difficulties.

Gravity stratification (Fig. 4) is encountered in all the above zones, but is most clearly distinquishable in the lower zone, where it generally takes the form of coarse-scale rhythmic layering, although in places it may also be manifest as fine-scale rhythmic layering or most often 'inch-scale' layering. Rhythmic layering tends to be coarser in character in the other zones, and is also less immediately observable. Igneous lamination, on the other hand, is most strikingly developed in the middle zone, and chiefly takes the form of plagioclase grain orientation. The above zonation, together with the occurrence of cumulus and intercumulus minerals and the variations in their composition, is depicted in Fig. 5.

The rocks of the lower zone are plagioclase-olivine-orthopyroxene mesocumulates or adcumulates with Ca-rich clinopyroxene and iron-titanium oxides, mainly ilmenite, as intercumulus crystals. Biotite is another common intercumulus mineral, frequently occurring in conjunction with ilmenite. Pronounced adcumulus growth is typical of many of the rocks in this zone.

In the middle zone olivine is no longer formed as a cumulus mineral, and the bronzite appearing in the lower zone is replaced by inverted pigeonite, while augite begins to crystallize as a cumulus mineral. The rocks of this zone are generally plagioclase-inverted pigeonite-augite orthocumulates or mesocumulates, that is norites or gabbronorites in their mineral composition. Adcumulus growth occurs to a very much smaller extent than in the lower zone. Quartz, which also frequently forms micropegmatitic intergrowths with alkali feldspar, is now a typical intercumulus mineral.

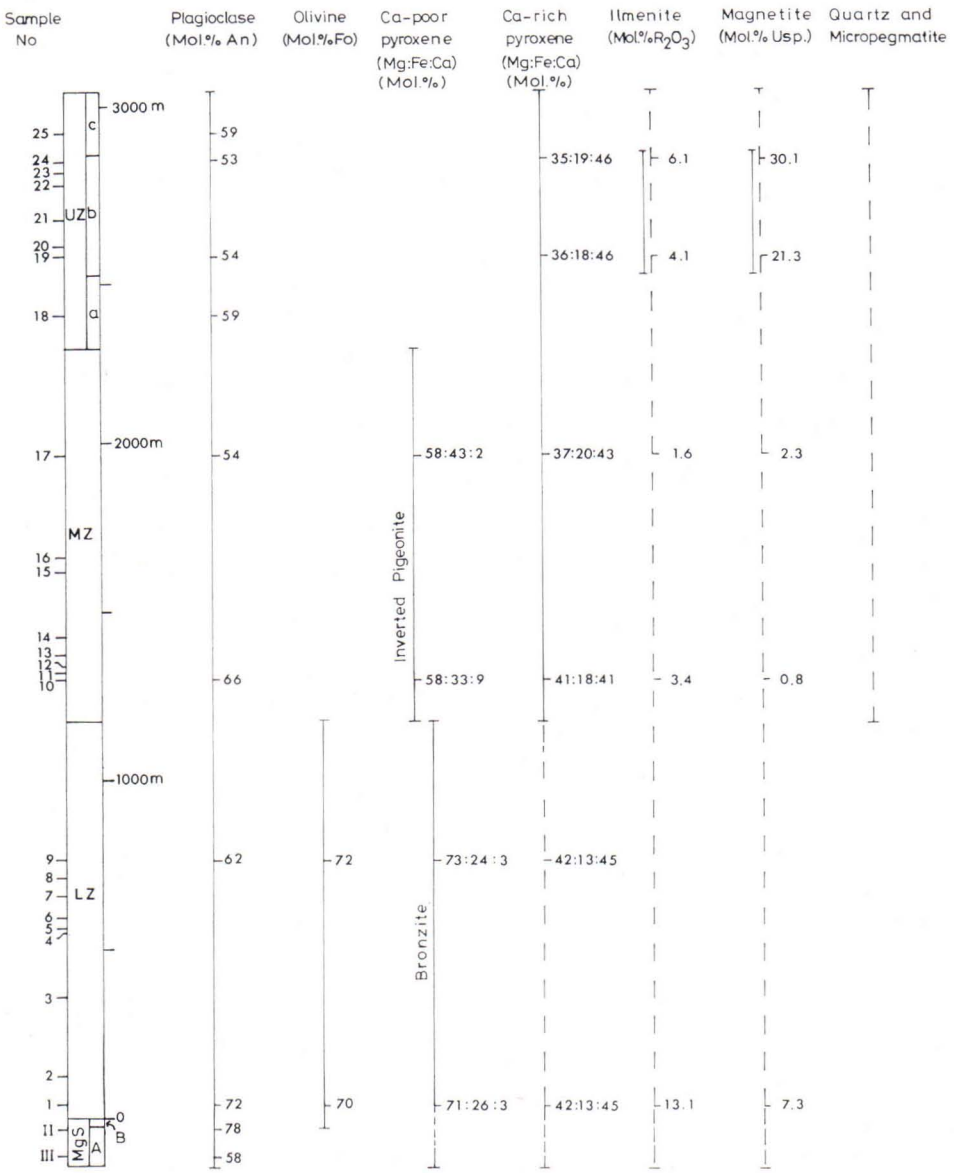

Fig. 5. Stratigraphic sequence and cryptic variation in minerals in the Syöte marginal and layered series. MgS, marginal series (A, contact gabbro; B, metaperidotite); LZ, lower zone; MZ, middle zone; UZ, upper zone (a and c, leucogabbros and anorthosites; b, magnetite gabbro). Intercumulus minerals are indicated by broken lines and cumulus minerals by solid lines.

The upper zone is the most heterogeneous of the three, and may conveniently be subdivided into three subzones a, b and c. Subzones a and c, the lowermost and uppermost horizons respectively, are formed chiefly of plagioclase-augite meso-

cumulates or orthocumulates in which plagioclase clearly dominates. As a result of marked uralitization, no primary augite is encountered. The intercumulus material in these subzones is broadly similar to that found in the middle zone. These rocks are thus leucogabbros and in places anorthosites, subzone a most commonly featuring anorthositic gabbros and subzone c gabbroic anorthosites.

Between these plagioclase-rich subzones a and c is found a magnetite gabbro horizon which is designated here subzone b. Its constituent minerals are plagioclase, ilmenomagnetite and augite, which has generally been subject to pronounced uralitization. Judging from the pseudomorphs present, it is also probable that the magnetite gabbro may have contained inverted pigeonite, which is not encountered as a primary component. The magnetite gabbro contains very little pore material.

MINERALS OF THE SYÖTE SECTION

Olivine

Olivine is encountered only in the lower zone, where it occurs as a cumulus mineral along with plagioclase and bronzite. On account of the pronounced adcumulus growth it is often found as an entirely anhedral grain (Fig. 6). Its composition varies within relatively narrow limits, from approx. Fo_{73} to Fo_{68} (Table 2).

Fig. 6. An entirely anhedral grain of partly serpentinized olivine resulting from pronounced adcumulus growth. (Sample 3). Magn. 18X. Without analyzer.

Table 2.

Microprobe analyses of olivines, and number of cations on the basis of 4 oxygen atoms. (For sample classifications, see Table 1.)

	1	2	3	4	6	7	9
SiO_2	37.6	37.2	38.0	37.3	37.5	38.6	37.7
TiO_2	n.d.	n.d.	n.d.	n.d.	n.d.	n.d.	0.05
Al_2O_3	n.d.	n.d.	n.d.	n.d.	n.d.	n.d.	0.06
FeO	27.0	29.0	26.5	24.6	27.0	26.7	25.6
MnO	0.34	0.21	0.39	0.27	0.32	0.17	0.30
MgO	35.5	34.8	35.0	37.3	37.2	37.9	37.2
CaO	0.11	0.09	0.10	0.10	0.09	0.09	0.05
Total	100.6	101.3	100.0	99.6	102.1	103.5	101.0
Si	0.995	0.987	1.008	0.987	0.978	0.988	0.987
Al	—	—	—	—	—	—	0.002
Ti	—	—	—	—	—	—	0.001
Fe^{2+}	0.598	0.643	0.588	0.545	0.589	0.572	0.561
Mn	0.008	0.005	0.009	0.006	0.007	0.004	0.007
Mg	1.401	1.376	1.384	1.472	1.446	1.446	1.452
Ca	0.003	0.003	0.003	0.003	0.003	0.002	0.001
Mol. %							
Fo	70.1	68.1	70.2	73.0	71.1	71.7	72.1
Fa	29.9	31.9	29.8	27.0	28.9	28.3	27.9

n.d. = not determined (below limit of sensitivity 0.05 %).

Ca-poor pyroxene

Ca-poor pyroxene occurs as a cumulus mineral in the lower and middle zones, and probably also in the magnetite gabbro horizon. It was also a typical mineral in the marginal zone at the early stages of crystallization, but has since undergone complete uralitization.

The Ca-poor pyroxene in the lower zone takes the form of bronzite, and varies in composition within fairly narrow limits (Table 3). Here adcumulus growth has been pronounced, and the grains are consequently somewhat anhedral. Finescale exsolution lamellae of augite // (100) of the orthopyroxene host are typical of these bronzites.

Myrmekitic intergrowths of orthopyroxene and ilmenite are typical of the rocks of the lower horizons (Fig. 7.) Intergrowths of this kind are described by Frick (1973) in kimberlite from South Africa and Haselton & Nash (1975) in the Skaergaard intrusion and in rock samples from the moon.

The Ca-poor pyroxene in the middle zone crystallized originally as pigeonite, i.e. the crystallization has taken place in the area above the pigeonite—orthopyroxene inversion curve (Brown 1957). Typical of these pyroxenes are exsolution lamellae of augite parallel to the relict (001) plane of the original pigeonite (Fig. 8), while very thin lamellae // (100) of the orthopyroxene are also frequently to be found, which have exsolved after inversion to hypersthene. The inverted pigeonite

Table 3.

Microprobe analyses of orthopyroxenes, and number of cations on the basis of 6 oxygen atoms. (For sample classifications, see Table 1.)

	1	2	3	4	5	6	7	8	9	10	12	13	14	16	17
SiO_2	54.2	53.8	54.9	54.2	53.7	55.1	53.7	53.0	54.1	52.9	50.2	50.2	52.3	53.0	50.5
TiO_2	0.36	0.52	0.17	0.16	0.25	0.19	0.16	0.10	0.17	0.23	0.36	0.31	0.51	0.16	0.25
Al_2O_3	1.26	1.50	1.18	1.5	1.2	1.4	1.4	1.4	1.2	0.87	1.0	0.78	0.92	1.10	0.75
Cr_2O_3	n.d.	n.d.	n.d.	0.20	n.d.	0.10	0.10	0.14	n.d.	n.d.	n.d.	n.d.	n.d.	0.17	n.d.
FeO	16.7	17.7	14.1	13.7	18.8	16.0	15.6	14.8	15.8	23.2	22.4	23.9	22.3	21.8	26.3
MnO	0.31	0.34	0.31	0.27	0.43	0.28	0.29	0.28	0.31	0.49	0.46	0.44	0.32	0.41	0.50
MgO	26.3	25.2	26.4	29.5	26.9	27.5	27.5	25.1	27.4	22.3	21.4	20.0	23.9	23.3	19.2
CaO	1.5	2.2	2.08	0.84	1.7	1.6	2.8	2.2	1.5	1.8	1.7	1.8	1.8	1.7	0.86
Na_2O	n.d.	n.d.	n.d.	0.07	0.05	n.d.	n.d.	n.d.	n.d.	n.d.	n.d.	n.d.	0.06	n.d.	n.d.
Total	100.6	101.3	99.1	100.4	103.0	102.1	101.6	97.0	100.5	101.8	97.5	97.4	102.1	101.6	98.4
Si	1.957	1.944	1.987	1.934	1.918	1.952	1.923	1.973	1.950	1.951	1.936	1.951	1.919	1.945	1.959
Al^{IV}	0.043	0.056	0.013	0.063	0.051	0.048	0.059	0.027	0.050	0.038	0.045	0.036	0.040	0.048	0.034
Al^{VI}	0.010	0.008	0.037	—	—	0.010	—	0.034	0.001	—	—	—	—	—	—
Ti	0.010	0.014	0.005	0.004	0.007	0.005	0.004	0.003	0.005	0.006	0.010	0.009	0.014	0.004	0.007
Cr	—	—	—	0.006	—	0.003	0.003	0.004	—	—	—	—	—	0.005	—
Fe^{2+}	0.504	0.535	0.427	0.409	0.562	0.474	0.467	0.461	0.476	0.716	0.723	0.777	0.684	0.669	0.853
Mn	0.009	0.010	0.010	0.008	0.013	0.008	0.009	0.009	0.009	0.015	0.015	0.014	0.010	0.013	0.016
Mg	1.415	1.357	1.424	1.569	1.432	1.452	1.468	1.393	1.472	1.226	1.230	1.159	1.307	1.274	1.110
Ca	0.058	0.085	0.081	0.032	0.065	0.061	0.107	0.088	0.058	0.071	0.070	0.075	0.071	0.067	0.036
Na	—	—	—	0.005	0.003	—	—	—	—	—	—	—	0.004	—	—
Mol. %															
En	71.2	68.3	73.4	77.7	69.1	72.8	71.6	71.4	73.0	60.5	60.4	57.2	63.1	63.0	55.1
Fs	25.9	27.4	22.5	20.7	27.7	24.2	23.2	24.1	24.1	36.0	36.2	39.1	33.5	33.7	43.1
Wo	2.9	4.3	4.2	1.6	3.1	3.0	5.2	4.5	2.9	3.5	3.4	3.7	3.4	3.3	1.8
100 Mg/(Mg+Fe+Mn)	73.4	71.3	76.5	79.0	71.4	75.1	75.5	74.8	75.2	62.9	62.5	59.4	65.3	65.1	56.1

n.d. = not determined (below limit of sensitivity 0.05 %).

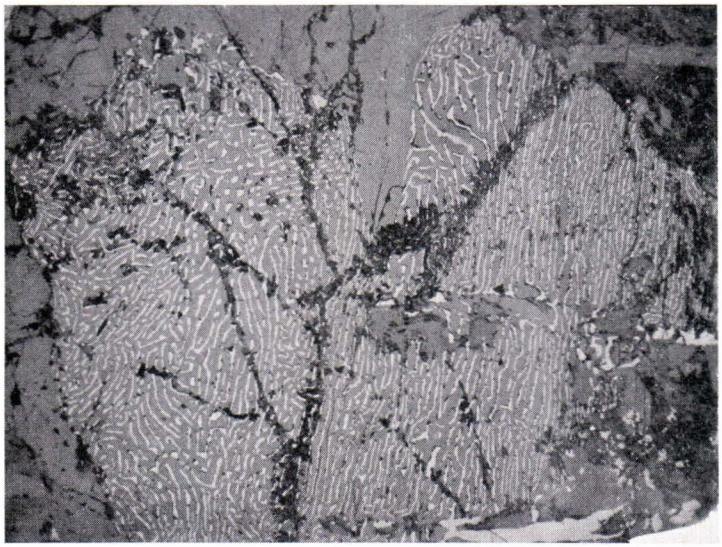

Fig. 7. Intergrowth of orthopyroxene and ilmenite in the lower zone. Magn. 70X.

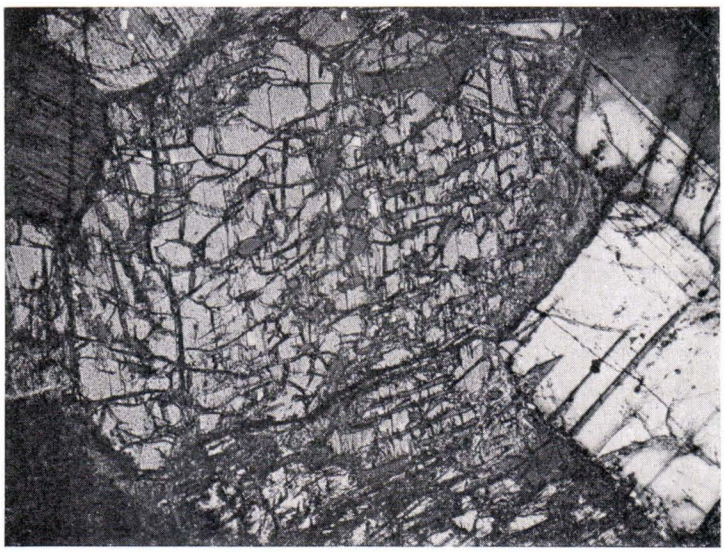

Fig. 8. Inverted pigeonite from the middle zone (Sample 10) showing broad exsolution lamellae of augite parallel to the relict (001) plane of original pigeonite. Magn. 36X. Crossed nicols.

Table 4.

Microprobe analysis of an exsolved augite lamellae (1) in inverted pigeonite, and calculated composition of the original pigeonite (2), sample no. 10.

	1	2
SiO_2	51.8	51.88
TiO_2	0.57	0.28
Al_2O_3	1.70	0.97
FeO	10.9	21.07
MnO	0.28	0.45
MgO	14.9	20.87
CaO	20.0	4.43
Na_2O	0.35	0.05
Total	100.5	100.00

sample, no. 10 (Fig. 8), which represents the lowest horizon encountered in the middle zone, contained (by point counter analysis) 15 % augite exsolution lamellae parallel to the relict (001) plane of pigeonite, the composition of which is detailed in Table 4. Since the composition of the orthopyroxene host was also known (Table 3), it then became possible to calculate fairly accurately the composition of the original pigeonite.

Ca-rich pyroxene

Unaltered Ca-rich pyroxene was encountered in the lower and middle zones and the magnetite gabbro horizon of the upper zone, and judging from its pseudomorphs it must also have been a typical mineral in the leucogabbro horizons and the marginal zone, having subsequently undergone complete uralitization. These Ca-rich pyroxenes correspond to augite in their composition (Table 5), but since it is generally only the augite host which it is possible to analyse, their Ca content will be somewhat overestimated.

In the lower zone this augite occurs as an intercumulus mineral and is generally clearly poikilitic in texture. It normally encloses orthopyroxene lamellae running parallel to the (100) plane of the augite host, although sometimes these may be found to be parallel to both the (100) and (001) planes, and very occasionally to the (001) plane alone.

Ca-rich pyroxene appears in the middle zone as a cumulus mineral, crystallizing at a temperature above the pigeonite—orthopyroxene inversion curve, and thus containing pigeonite lamellae parallel to the (001) plane of the augite host. These lamellae form a herringbone pattern in twinned augites (Fig. 9). (100)-lamellae are also visible at times, since the exsolved pigeonite has itself inverted to orthopyroxene. Only (001)-lamellae are to be found in the augites of the magnetite gabbro horizon.

Table 5.

Microprobe analyses of clinopyroxenes, and number of cations on the basis of 6 oxygen atoms. (For sample classifications, see Table 1.)

	1	2	3	4	5	6	7	8	9	10	11	12
SiO_2	52.1	52.3	51.5	51.0	50.9	51.5	51.5	50.1	50.2	51.9	50.9	49.1
TiO_2	0.58	0.88	0.40	0.30	0.35	0.40	0.31	0.88	0.60	0.68	0.50	0.62
Al_2O_3	2.1	2.6	2.1	2.1	2.4	2.2	2.2	2.9	3.1	1.9	1.8	1.9
Cr_2O_3	0.11	n.d.	0.10	0.18	n.d.	0.11	0.09	n.d.	n.d.	n.d.	0.11	n.d.
FeO	8.0	8.4	8.4	7.6	8.5	7.5	8.1	8.7	7.7	11.5	11.7	11.3
MnO	0.21	0.27	0.21	0.12	0.22	0.14	0.12	0.19	0.16	0.29	0.29	0.18
MgO	14.7	14.3	14.5	15.0	16.0	15.6	16.0	13.7	14.8	14.6	14.3	12.7
CaO	22.3	21.6	20.6	21.0	23.0	22.2	21.0	20.3	22.3	20.2	20.3	20.3
Na_2O	0.18	0.21	0.18	0.43	0.42	0.30	0.39	0.39	0.33	0.35	0.18	0.20
Total	100.3	100.6	98.0	97.7	101.8	100.0	99.7	97.2	99.2	101.4	100.1	96.3
Si	1.932	1.932	1.950	1.935	1.876	1.915	1.918	1.919	1.887	1.925	1.919	1.926
Al^{IV}	0.068	0.068	0.050	0.065	0.104	0.085	0.082	0.081	0.113	0.075	0.080	0.074
Al^{VI}	0.024	0.045	0.043	0.029	—	0.012	0.015	0.050	0.024	0.008	—	0.014
Ti	0.016	0.024	0.011	0.009	0.010	0.011	0.009	0.025	0.017	0.019	0.014	0.018
Cr	0.003	—	0.003	0.005	—	0.003	0.003	—	—	—	0.003	—
Fe^{2+}	0.248	0.259	0.266	0.241	0.262	0.233	0.252	0.279	0.242	0.357	0.369	0.371
Mn	0.007	0.008	0.007	0.004	0.007	0.004	0.004	0.006	0.005	0.009	0.009	0.006
Mg	0.813	0.787	0.818	0.848	0.879	0.865	0.888	0.782	0.829	0.807	0.804	0.742
Ca	0.886	0.855	0.836	0.854	0.908	0.885	0.838	0.833	0.898	0.803	0.820	0.853
Na	0.013	0.015	0.013	0.032	0.030	0.022	0.028	0.029	0.024	0.025	0.013	0.015
Mol. %												
En	41.6	41.2	42.5	43.6	42.7	43.5	44.8	41.2	42.0	40.9	40.1	37.6
Fs	13.0	14.0	14.2	12.6	13.1	12.0	12.9	15.0	12.5	18.5	18.9	19.1
Wo	45.4	44.8	43.4	43.8	44.2	44.5	42.3	43.8	45.5	40.6	41.0	43.3
100 Mg/ (Mg+Fe+Mn)	76.1	74.6	75.0	77.6	76.6	78.4	77.6	73.3	77.0	68.8	68.0	66.3

Fig. 9. Exsolution lamellae of pigeonite in twinned augite parallel to (001) plane of augite host forming the herringbone pattern. Middle zone sample 11. Magn. 60X. Crossed nicols.

Table 5. Clinopyroxene analyses — continued.

	13	14	15	16	17	19	20	21	22	23	24
SiO_2	48.8	50.7	51.5	50.2	49.2	49.3	49.0	47.3	50.6	49.5	48.7
TiO_2	0.64	0.32	0.48	0.74	0.15	0.63	0.46	0.47	0.50	0.40	0.58
Al_2O_3	1.7	2.2	2.2	2.0	0.73	3.1	2.2	1.7	2.2	1.6	1.9
Cr_2O_3	0.18	0.08	n.d.	n.d.	n.d.	n.d.	n.d.	n.d.	n.d.	n.d.	n.d.
FeO	11.5	9.8	11.6	11.6	11.9	11.3	11.5	10.7	11.0	12.0	12.1
MnO	0.31	0.21	0.17	0.27	0.27	0.25	0.21	0.26	0.31	0.25	0.34
MgO	13.1	14.7	14.3	13.7	12.8	12.7	12.6	13.3	11.7	13.4	12.4
CaO	20.5	22.5	20.8	21.0	20.8	22.5	22.0	22.9	21.0	22.0	22.8
Na_2O	0.22	0.20	0.34	n.d.	0.18	0.58	0.39	0.42	0.45	0.41	0.53
Total	97.0	100.7	101.4	99.5	96.0	100.4	98.4	97.1	97.8	99.6	99.4
Si	1.909	1.896	1.915	1.908	1.947	1.869	1.895	1.864	1.950	1.896	1.880
Al^{IV}	0.078	0.097	0.085	0.090	0.034	0.131	0.100	0.079	0.050	0.072	0.086
Al^{VI}	—	—	0.011	—	—	0.007	—	—	0.050	—	—
Ti	0.019	0.009	0.013	0.021	0.004	0.018	0.013	0.014	0.014	0.012	0.017
Cr	0.006	0.002	—	—	—	—	—	—	—	—	—
Fe^{2+}	0.376	0.306	0.361	0.369	0.394	0.358	0.372	0.353	0.355	0.384	0.391
Mn	0.010	0.007	0.005	0.009	0.009	0.008	0.007	0.009	0.010	0.008	0.011
Mg	0.764	0.819	0.792	0.776	0.755	0.718	0.726	0.781	0.672	0.765	0.713
Ca	0.859	0.901	0.829	0.855	0.882	0.914	0.912	0.967	0.867	0.903	0.943
Na	0.017	0.015	0.025	—	0.014	0.043	0.029	0.032	0.034	0.030	0.040
Mol. %											
En	38.0	40.3	39.9	38.6	37.0	35.9	36.0	37.0	35.3	37.1	34.7
Fs	19.2	15.4	18.4	18.8	19.8	18.3	18.8	17.1	19.2	19.1	19.5
Wo	42.8	44.3	41.7	42.6	43.2	45.7	45.2	45.8	45.5	43.8	45.8
100 Mg/(Mg+Fe+Mn)	66.4	72.4	68.4	67.3	65.2	66.2	65.7	68.4	64.8	66.1	64.0

n.d. = not determined (below limit of sensitivity 0.05 %).

Table 6.

Composition of plagioclases in the Syöte marginal and layered series. (For sample classifications, see Table 1.)

	II	III	1	2	3	4	5	6	7	8	9	10	11	12
An (mol. %)	77.5	58.0	71.7	80.8	72.3	74.8	69.6	59.2	63.1	72.5	62.1	66.4	63.7	62.1
Ab (mol. %)	21.0	41.2	26.6	18.1	26.6	24.4	28.0	39.3	36.6	27.3	35.7	32.3	35.0	36.6
Or (mol. %)	1.5	0.8	1.7	1.1	1.2	0.8	2.4	1.5	0.3	0.2	2.1	1.2	1.3	1.3
Fe (wt %)	0.47	0.36	0.33	0.34	0.45	0.26	0.39	0.30	0.32	0.31	0.34	0.44	0.43	0.31

Table 6. Composition of plagioclases — continued.

	13	14	15	16	17	18	19	20	21	22	23	24	25
An (mol. %)	68.6	58.1	62.1	64.6	53.5	58.6	53.5	56.0	54.0	57.5	53.4	52.7	58.8
Ab (mol. %)	30.0	40.9	37.3	34.4	46.1	39.1	44.8	42.0	43.6	40.7	44.5	45.0	40.6
Or (mol. %)	1.4	1.0	0.6	1.0	0.4	2.3	1.6	2.0	2.4	1.8	2.1	2.3	0.6
Fe (wt. %)	0.43	0.37	0.42	0.40	0.37	0.45	0.55	0.55	0.55	0.51	0.56	0.48	0.35

Table 7.

Microprobe analyses of Fe-Ti-oxides. (For sample classifications, see Table 1.)

Spinel phase	1*	2***	3**	5***	6	10***	11**	12***	14***
SiO_2	0.10	n.d.	n.d.	2.0	—	0.07	n.d.	n.d.	0.2
TiO_2	2.39	0.70	0.30	0.13	—	0.19	0.22	0.26	1.1
Al_2O_3 ...	0.11	0.46	1.1	0.85	—	n.d.	0.05	0.13	0.07
Cr_2O_3 ...	0.11	n.d.	n.d.	n.d.	—	0.34	0.13	0.33	0.28
V_2O_3	1.0	0.60	1.1	0.84	—	1.0	1.0	1.1	1.1
FeO	89.5	88.3	92.2	84.8	—	91.4	94.3	92.4	87.4
MnO	0.11	n.d.	0.76	0.08	—	n.d.	0.10	n.d.	0.13
MgO	0.15	0.08	0.22	3.0	—	0.21	n.d.	n.d.	n.d.
CaO	n.d.	n.d.	n.d.	0.22	—	n.d.	n.d.	n.d.	n.d.
Sum	93.5	90.1	95.7	91.9	—	93.2	95.8	94.2	90.3
Recalculated analyses (after Carmichael 1967).									
Ilmenite basis									
Fe_2O_3 ...	64.5	64.7	68.0	64.5	—	67.3	69.4	67.7	63.4
FeO	31.5	30.1	31.0	26.8	—	30.8	31.9	31.5	30.3
Total	100.0	96.6	102.5	98.4	—	99.9	102.8	101.0	96.6
Ulvospinel basis									
Fe_2O_3 ...	62.8	64.2	67.8	62.6	—	67.1	69.2	67.5	62.5
FeO	33.0	30.5	31.2	28.5	—	31.0	32.0	31.6	31.2
Total	99.8	96.5	102.5	98.2	—	99.9	102.7	100.9	96.6
Mol. % Usp. ..	7.3	2.1	0.8	7.9	—	0.8	0.6	0.7	4.0

Rhombohedral phase	1	2	3	5	6	10	11	12	14
SiO_2	n.d.	n.d.	n.d.	0.08	n.d.	0.09	n.d.	n.d.	n.d.
TiO_2	46.7	42.0	49.8	52.9	52.5	51.5	51.8	51.6	51.1
Al_2O_3 ...	0.06	3.4	n.d.	0.06	0.06	0.06	n.d.	n.d.	n.d.
Cr_2O_3 ...	n.d.	n.d.	n.d.	0.05	n.d.	0.05	0.05	n.d.	0.11
V_2O_3	0.21	0.20	0.26	0.21	0.40	0.23	0.34	0.22	0.25
FeO	52.1	47.4	47.4	47.9	48.2	45.6	47.7	45.1	46.8
MnO	1.1	1.3	1.50	1.70	0.82	0.80	1.60	2.10	1.10
MgO	0.65	3.4	1.0	0.08	0.17	0.10	0.08	0.11	0.11
CaO	n.d.	0.05	n.d.	n.d.	n.d.	n.d.	n.d.	n.d.	n.d.
Sum	100.8	97.8	100.0	103.0	102.1	98.4	101.6	99.1	99.5
Recalculated analyses (after Carmichael 1967).									
Fe_2O_3 ...	13.8	19.0	6.6	2.3	2.4	0.2	3.2	1.1	2.4
FeO	39.8	30.3	41.5	45.2	46.1	45.4	44.8	44.1	44.6
Total	102.2	99.7	100.6	103.2	102.4	98.4	102.0	99.2	99.7
Mol. % R_2O_3 ..	13.1	22.6	6.4	2.5	2.7	0.6	3.4	1.3	2.7
Temp. °C	600	~600	< 600	< 600	—	—	—	—	< 550
f_{O_2}	$10^{-18.5}$	< 10^{-20}	< 10^{-20}	< 10^{-20}	—	—	—	—	< 10^{-20}

n.d. = not determined (below limit of sensitivity 0.05 %).
* Titaniferous magnetite and discrete ferrian ilmenite.
** Ilmeno-magnetite and ferrian ilmenite in composite grains.
*** Host titaniferous magnetite and ferrian ilmenite lamellae.
Temperatures and oxygen fugacities were determined from the T-f_{O_2}-X data of Buddington and Lindsley (1964).

Table 7.

Microprobe analyses of Fe-Ti-oxides — continued.

Spinel phase	16**	17**	19**	20**	21**	22**	23**	24**
SiO_2	n.d.	0.05	n.d.	0.06	0.09	0.09	0.06	0.18
TiO_2	0.76	0.75	7.40	10.0	7.59	10.3	11.6	10.4
Al_2O_3 ...	0.23	0.10	0.11	0.10	0.15	0.17	0.19	0.18
Cr_2O_3 ...	0.20	n.d.	n.d.	n.d.	n.d.	n.d.	0.06	n.d.
V_2O_3	1.1	1.2	1.50	1.60	1.13	1.17	1.60	1.53
FeO	90.1	91.7	85.1	82.7	83.6	83.9	80.2	83.5
MnO	n.d.	0.36	0.33	0.49	0.39	0.19	0.59	0.63
MgO	0.08	0.11	0.08	0.05	0.05	0.07	n.d.	n.d.
CaO	n.d.	n.d.	n.d.	n.d.	0.05	n.d.	n.d.	n.d.
Sum	92.5	94.3	94.5	95.0	93.1	95.9	94.3	96.4
Recalculated analyses (after Carmichael 1967).								
Ilmenite basis								
Fe_2O_3 ...	65.8	67.3	57.9	54.3	56.8	55.0	51.4	54.6
FeO	30.9	31.1	33.0	33.8	32.5	34.5	33.9	34.4
Total	99.1	101.0	100.3	100.4	98.7	101.3	99.5	101.9
Ulvospinel basis								
Fe_2O_3 ...	65.3	66.8	53.0	47.7	51.6	48.0	43.7	47.5
FeO	31.4	31.6	37.5	39.8	37.1	40.7	40.9	40.7
Total	99.1	101.0	99.8	99.8	98.2	100.7	98.7	101.1
Mol. % Usp. ..	2.2	2.3	21.3	28.9	22.5	29.6	33.8	30.1

Rhombohedral phase	16	17	19	20	21	22	23	24
SiO_2	0.07	0.09	0.06	n.d.	0.08	0.05	n.d.	n.d.
TiO_2	51.4	51.0	50.7	50.5	52.3	50.8	48.1	49.7
Al_2O_3 ...	n.d.	n.d.	n.d.	n.d.	0.07	n.d.	n.d.	n.d.
Cr_2O_3 ...	0.05	n.d.	n.d.	n.d.	n.d.	n.d.	n.d.	n.d.
V_2O_3	0.25	0.36	0.30	n.d.	0.40	0.21	0.39	0.39
FeO	45.4	45.2	46.0	46.3	47.3	46.4	48.5	47.6
MnO	1.30	1.65	2.93	0.11	1.86	2.02	2.36	2.25
MgO	0.10	0.15	0.16	0.14	0.14	0.13	0.08	0.11
CaO	n.d.	n.d.	0.05	n.d.	n.d.	n.d.	n.d.	n.d.
Sum	98.6	98.5	100.2	97.1	102.1	99.6	99.4	100.1
Recalculated analyses (after Carmichael 1967).								
Fe_2O_3 ...	0.7	1.3	4.1	1.4	2.6	3.3	8.6	6.0
FeO	44.8	44.0	42.3	45.1	45.0	43.5	40.7	42.2
Total	98.6	98.6	100.6	97.2	102.4	99.9	100.3	100.6
Mol. % R_2O_3 ..	0.9	1.6	4.1	1.4	2.9	3.3	8.6	6.1
Temp. °C	—	—	650	< 600	630	680	790	740
f_{O_2}	—	—	10^{-19}	$< 10^{-20}$	10^{-20}	10^{-18}	$10^{-14.5}$	10^{-16}

Plagioclase

Cumulus plagioclase is met with throughout the exposed layered series, and the same mineral is also typical of the 'contact gabbro' of the marginal series. The plagioclase samples analysed vary in composition from approx. An_{80} to An_{50}, and even adjacent samples may deviate markedly in this respect (Table 6). Ca, Na and K analyses were performed on plagioclase grains, enabling their An, Ab and Or content to be calculated, an attempt being made to use in these analyses the central part of the grain, that richest in Ca. An analysis was also carried out of the Fe content, which appears broadly speaking to show a negative correlation with the anorthite content.

Some zonation is commonly to be found in the cumulus plagioclase grains, especially in the lower parts of the sequence, and the composition of the adcumulus material is not identical in every case with the probable original cumulus crystal, which is frequently to be seen, tabular in shape, at the grain centre.

Iron-titanium oxides

Iron-titanium oxides containing vanadium (Table 7) occur throughout the area of the section, even forming the constituent minerals in the magnetite gabbro. The ilmeno-magnetites of the marginal series have undergone pronounced alteration, and now appear as skeletal relicts among the plagioclase and uralite, in many places in the contact gabbro (cf. Piirainen *et al.* 1977).

The typical iron-titanium oxide minerals in the layered series consist of a titaniferous magnetite host with ferrian ilmenite lamellae running parallel to the {111} of the ilmeno-magnetite, intergrown with a coarse, relatively homogeneous ferrian ilmenite to form a composite ilmeno-magnetite-ferrian ilmenite grain (Fig. 10). Less ilmenite lamellae are to be found in the magnetite gabbro horizon, while the proportion of coarser ilmenite is greater than in the lower and middle zones.

Discrete ferrian ilmenite is encountered in the lower and middle zones, and this even becomes more frequent than the composite ilmeno-magnetite-ferrian ilmenite grains in the lowermost horizons of the lower zone. These discrete ferrian limenite grains often occur together with biotite as intercumulus minerals, and in the lower horizons they also form myrmekitic intergrowths with orthopyroxene (see p. 14). The titaniferous magnetite host of the ilmeno-magnetites in the lower and middle zones is often transformed into a silicate, either biotite or amphibole, or both, but the ilmenite lamellae running parallel to the relict {111} of the original ilmento-magnetite have been preserved entirely unaltered.

Fig. 10. Ilmeno-magnetite (1), consisting of ferrian ilmenite lamellae parallel to {111} in a titaniferous magnetite host, and forming a composite grain with coarse, irregular ferrian ilmenite (2). The ilmeno-magnetite also contains small inclusions of chalcopyrite (white). On the left is seen an intergrowth of orthopyroxene and ilmenite. Lower zone, sample 2. Magn. 70X.

Garnet

The lower zone also features in places an unusual brownish garnet with an exceptional isomorphous substitution between Fe^{2+} and Ca. This same garnet is also described by Mäkelä (1975) in the Porttivaara section. It occurs in small roundish or slightly elongated grains (< 0.5 mm) which are regularly enclosed in plagioclase (Fig. 11). Frequently they are found to have been altered to form an isotropic saussurite-like mass. The composition of this garnet is shown in Table 8. Since this analysis was carried out using a microprobe, the ferric iron content was not determined, but in view of the high aluminium content, it is clear that the ferric iron content cannot be very great, and thus the proportion of andradite would remain small, so that this garnet is chiefly a mixture of almandine and grossular.

Other minerals

Quartz is found as an intercumulus mineral in the middle and upper zones, and may be either in the form of independent grains or else micropegmatitic intergrowths with alkali feldspar. The greatest abundance of independent quartz and micropegmatitic intergrowths is to be found in the orthocumulates and mesocumulates of the middle zone.

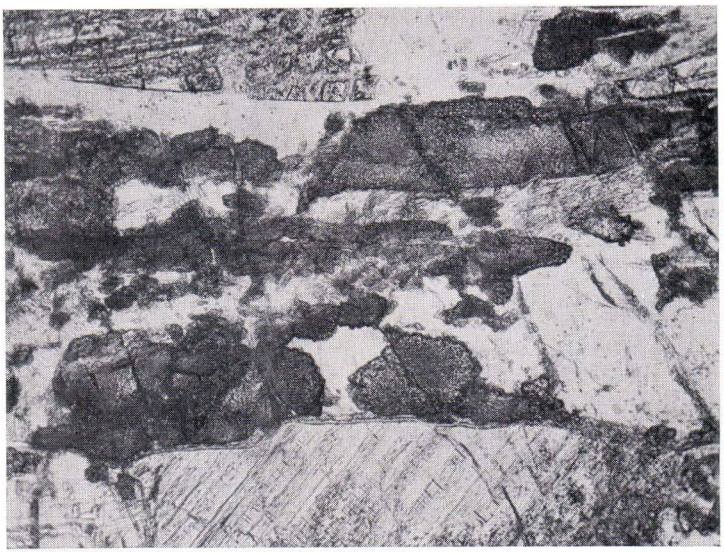

Fig. 11. Slightly elongated grains of garnet enclosed in plagioclase. Lower zone, sample 6. Magn. 60X. Without analyser.

Table 8.

Microprobe analysis of garnet, and number of cations on the basis of 24 oxygen atoms. Sample 6.

SiO_2	35.5	Si	5.671	6.00	Almandine	38.5
TiO_2	< 0.05	Al	0.329		Grossular	49.6
Al_2O_3	21.7				Pyrope	7.3
Cr_2O_3	< 0.05	Al	3.757		Spessartine	4.6
FeO_{tot}	18.8					
MnO	2.2	Fe^{2+}	2.512			
MgO	2.0	Mn	0.298			
CaO	18.9	Mg	0.476	6.54		
Na_2O	0.06	Ca	3.235			
K_2O	< 0.05	Na	0.019			
Total	99.2					

Cell edge 11.70±0.02 Å (Mäkelä 1975).

Zircon and apatite occur randomly in all horizons, together with the late crystallizing minerals from the trapped intercumulus liquid. Grains over one millimetre in size were even found in a few samples from the lower zone.

Biotite appears in the form of flakes in the lower zone, often in association with the iron-titanium oxides, especially ilmenite. Very much less is to be found in the middle zone, and it is a rare mineral in the upper zone.

Sulphides are found in traces throughout the intrusion, and their occurrence in the marginal zone is similar to that noted in the corresponding formation at Porttivaara (cf. Piirainen *et al.* 1977). The most commonly encountered sulphide

in the layered series is chalcopyrite, with pyrite, pyrrhotite, pentlandite, etc. also to be found. These sulphide minerals generally appear along with other late crystallizing minerals in the interspaces between the cumulus minerals. Chalcopyrite also occurs as a very fine-grained dissemination in augite or its alteration product uralite. This is especially common within the magnetite gabbro.

In addition, small quantities of chlorite, epidote, bluegreen clino-amphibole, etc. are to be found, either as final dregs of intercumulus liquid or as the hydrothermal alteration products of earlier minerals.

Table 9.

Chemical compositions of the Syöte marginal series, with C.I.P.W. norms (weight %). (For sample classifications, see Table 1.)

	I	II	III
SiO_2	44.24	46.52	48.08
TiO_2	0.17	0.15	0.20
Al_2O_3	7.50	16.87	16.23
Fe_2O_3	5.74	1.32	2.71
FeO	9.05	5.86	5.45
MnO	0.18	0.17	0.14
MgO	25.79	12.15	8.66
CaO	6.13	10.41	8.32
Na_2O	0.36	1.50	1.95
K_2O	0.00	0.33	1.59
P_2O_5	0.05	0.02	0.07
Total	99.21	95.30	93.40
Co (ppm)	120	60	120
Cr »	390	860	640
Cu »	220	180	290
Ni »	1 470	590	3 100
S »	400	300	10 300
Sr »	n.d.	300	600
V »	100	n.d.	n.d.
Zn »	70	60	80
or	—	2.11	9.78
pl	21.91	50.92	47.14
(an*)	(85.94)	(75.14)	(64.93)
di	8.94	10.60	8.15
hy	29.00	15.50	21.09
(en**)	(84.09)	(75.71)	(77.60)
ol	30.72	13.93	2.02
(fo***)	(82.75)	(73.87)	(75.87)
mt	8.35	1.91	3.93
il	0.32	0.29	0.38
ap	0.11	0.05	0.16
pr	0.07	0.06	1.93
Total	99.42	95.37	94.61
CI	69.02	65.05	50.14

n.d. = not detected
* wt % anorthite in plagioclase
** wt % enstatite in hypersthene
*** wt % forsterite in olivine
CI Crystallization index (Poldervaart & Parker 1964.)

Table 10.

Chemical compositions of the Syöte layered series, with C.I.P.W. norms and modes. (For sample classifications, see Table 1.)

	1	2	3	4	5	6	7	8	9
SiO_2	46.47	46.68	48.39	44.93	49.85	46.29	45.69	48.24	44.11
TiO_2	0.32	0.43	0.18	0.27	0.35	0.17	0.15	0.40	0.18
Al_2O_3 ...	16.71	17.54	17.42	14.26	24.93	14.50	15.30	20.84	12.85
Fe_2O_3 ...	2.13	3.85	2.57	2.67	0.72	3.24	2.71	1.10	4.30
FeO	9.34	8.28	7.94	7.77	3.34	8.32	9.28	5.52	9.23
MnO	0.21	0.18	0.19	0.22	0.09	0.23	0.22	0.13	0.25
MgO	15.40	13.30	13.80	17.50	4.50	16.40	16.80	8.60	19.80
CaO	8.79	7.50	8.94	6.91	13.90	8.03	8.49	11.05	6.42
Na_2O ...	1.44	1.55	1.54	1.00	2.86	0.98	1.28	2.28	1.13
K_2O	0.31	0.27	0.20	0.48	0.41	0.18	0.14	0.37	0.16
P_2O_5	0.02	0.05	n.d.	0.02	n.d.	n.d.	n.d.	0.02	n.d.
H_2O^+ ...	1.60	2.80	1.90	4.10	0.90	3.20	2.20	2.00	2.70
H_2O^- ...	0.06	0.11	0.09	0.16	0.04	0.04	0.06	0.04	0.09
Total	102.80	102.54	103.17	100.29	101.89	101.58	102.33	100.59	101.21

n.d. = not detected

C.I.P.W. Norms (weight %)

q	—	—	—	—	—	—	—	—	—
or	1.83	1.60	1.18	2.84	2.42	1.06	0.83	2.19	0.95
pl	50.40	50.00	53.06	41.47	75.90	42.93	46.42	64.83	39.08
an*	(75.82)	(73.77)	(75.44)	(79.59)	(71.12)	(80.68)	(76.67)	(70.24)	(75.53)
c	—	1.18	—	—	—	—	—	—	—
ne	—	—	—	—	1.23	—	—	—	—
di	4.23	—	3.47	0.91	12.10	4.16	5.24	7.37	1.86
hy	13.43	28.99	24.42	24.21	—	28.81	15.31	9.03	19.64
en**	(71.55)	(73.98)	(73.31)	(78.38)	—	(76.21)	(73.66)	(70.86)	(78.43)
ol	27.50	11.35	14.97	22.18	7.59	16.36	28.05	12.74	30.33
fo*** ...	(69.53)	(72.07)	(71.37)	(76.68)	(66.48)	(74.41)	(71.73)	(68.81)	(76.74)
mt	3.09	5.58	3.73	3.87	1.04	4.70	3.93	1.59	6.23
ap	0.05	0.12	—	0.05	—	—	—	0.05	—
il	0.61	0.82	0.34	0.51	0.66	0.32	0.28	0.76	0.34
Total	101.14	99.63	101.17	96.03	100.95	98.34	100.06	98.55	98.43
CI	65.38	58.60	63.87	63.86	66.41	64.45	66.07	63.87	64.30

* wt % anorthite in plagioclase
** wt % enstatite in hypersthene
*** wt % forsterite in olivine
CI Crystallization index (Poldervaart & Parker 1964).

Modes (vol. %)

Ol	12.6	31.5	7.9	16.1	—	11.6	27.1	—	34.0
Opx	5.4	4.0	14.5	5.6	3.3	20.2	14.3	30.9	19.7
Cpx	25.5	7.1	18.6	10.7	15.2	13.4	17.5	trace	0.9
Pl	54.4	56.3	59.0	67.6	78.9	54.6	41.0	68.9	45.3
Bi	—	—	—	—	1.4	—	—	—	—
Q	—	—	—	—	—	—	—	—	—
Fe-Ti-Ox	—	—	—	—	0.6	—	—	—	—
Others ..	0.1	1.1	—	—	0.6	0.2	0.1	0.2	0.1
	100.0	100.0	100.0	100.0	100.0	100.0	100.0	100.0	100.0

Ol Olivine+skeletal pseudomorphs of olivine
Opx Orthopyroxene+uralite (pseudomorph of orthopyroxene)
Cpx Clinopyroxene+uralite (pseudomorph of clinopyroxene)
Pl Plagioclase
Bi Biotite
Q Quartz and micropegmatitic intergrowths
Fe-Ti-Ox Ilmenomagnetite and ilmenite

Table 10. Chemical compositions — continued.

	10	11	12	13	14	15	16	17
SiO_2	50.81	52.18	51.25	51.08	52.69	49.84	49.99	51.68
TiO_2	0.32	0.52	0.43	0.55	0.42	0.43	0.55	0.47
Al_2O_3 ...	20.31	21.76	19.65	18.11	21.32	17.20	20.38	18.04
Fe_2O_3 ...	1.74	2.07	1.63	1.63	1.66	1.70	1.90	2.50
FeO	5.96	4.31	6.01	6.87	5.40	7.51	6.47	7.14
MnO	0.17	0.14	0.17	0.19	0.15	0.19	0.17	0.21
MgO	6.60	4.90	6.60	6.90	6.40	7.20	6.20	6.70
CaO	11.80	11.76	11.94	12.10	11.92	11.90	10.67	11.37
Na_2O ...	2.51	2.97	2.43	2.22	2.63	2.26	2.37	2.67
K_2O	0.30	0.54	0.34	0.43	0.36	0.27	0.36	0.27
P_2O_5	n.d.	0.05	n.d.	0.05	0.06	n.d.	0.05	0.05
H_2O^+ ...	0.70	1.10	0.80	1.20	0.80	1.50	1.20	0.90
H_2O^- ...	0.04	0.03	0.04	0.04	0.05	0.02	0.08	0.06
Total	101.25	102.33	101.28	101.38	103.83	100.03	100.39	102.03

C.I.P.W. Norms (weight %)

q	—	0.85	—	0.22	0.24	—	0.32	0.34
or	1.77	3.19	2.01	2.54	2.13	1.60	2.13	1.60
pl	64.50	69.58	62.27	56.97	67.56	55.11	63.96	58.99
an*	(67.07)	(63.88)	(66.98)	(67.02)	(67.06)	(65.30)	(68.65)	(61.85)
c	—	—	—	—	—	—	—	—
ne	—	—	—	—	—	—	—	—
di	12.41	10.96	14.24	17.54	11.10	18.82	7.09	15.98
hy	16.06	12.52	18.60	19.35	18.69	16.80	21.70	19.55
en**	(63.88)	(68.52)	(63.88)	(61.60)	(66.22)	(59.85)	(61.37)	(61.02)
ol	2.64	—	0.15	—	—	2.89	—	—
fo*** ...	(61.61)	—	(61.61)	—	—	(57.50)	—	—
mt	2.52	3.00	2.36	2.36	2.41	2.46	2.75	3.62
ap	—	0.12	—	0.12	0.05	—	0.12	0.12
il	0.61	0.99	0.82	1.04	0.80	0.82	1.04	0.89
Total	100.52	101.20	100.45	100.13	102.97	98.50	99.11	101.09
CI	59.64	56.96	58.90	57.11	59.39	56.56	57.59	54.00

Modes (vol. %)

Ol	—	—	—	—	—	—	—	—
Opx	16.0	—	20.5	8.8	7.1	2.1	6.3	10.4
Cpx	17.9	23.8	19.4	48.7	16.5	29.7	9.5	37.4
Pl	65.3	69.9	57.2	37.9	72.6	65.0	79.2	49.5
Bi	—	1.6	0.6	0.9	0.5	1.7	—	—
Q	0.8	2.8	2.0	2.0	2.6	1.5	4.4	1.9
Fe-Ti-Ox	—	1.8	—	0.9	0.7	—	—	0.7
Others ..	—	0.1	0.3	0.8	—	—	0.6	0.1
	100.0	100.0	100.0	100.0	100.0	100.0	100.0	100.0

Table 10. Chemical compositions — continued.

	18	19	20	21	22	23	24	25
SiO_2	54.56	43.67	43.93	45.28	45.66	43.64	46.01	52.50
TiO_2	0.32	2.10	1.93	1.82	1.43	2.34	1.63	0.50
Al_2O_3 ...	25.11	14.80	14.92	14.62	14.56	15.33	15.20	22.57
Fe_2O_3 ...	1.57	9.28	8.51	7.52	6.49	8.94	6.53	2.33
FeO	1.70	11.09	10.93	11.22	9.74	11.59	9.97	4.30
MnO	0.04	0.21	0.21	0.21	0.18	0.19	0.19	0.10
MgO	1.04	6.40	7.10	6.90	6.90	6.70	6.20	3.64
CaO	11.15	10.62	10.60	10.88	11.69	10.22	11.35	9.92
Na_2O ...	3.85	1.87	1.85	1.97	1.79	1.99	1.99	4.02
K_2O	0.22	0.17	0.17	0.17	0.35	0.17	0.17	0.36
P_2O_5	0.02	n.d.	n.d.	n.d.	n.d.	n.d.	n.d.	0.09
H_2O^+ ...	1.30	1.40	1.40	1.60	1.80	1.40	1.70	2.30
H_2O^-	—	0.03	0.04	0.02	0.02	0.06	0.05	—
Total	100.66	101.64	101.59	102.20	100.62	102.57	101.01	102.27

C.I.P.W. Norms (weight %)

q	6.31	0.04	—	—	—	—	0.65	0.21
or	1.30	1.00	1.00	1.00	2.07	1.00	1.00	2.13
pl	83.16	47.31	47.56	47.22	45.81	49.23	48.88	76.49
an*	(60.83)	(66.55)	(67.09)	(64.70)	(66.93)	(65.80)	(65.55)	(55.53)
c	—	—	—	—	—	—	—	—
ne	—	—	—	—	—	—	—	—
di	3.73	17.26	16.82	19.15	22.26	14.92	19.83	5.00
hy	2.15	17.15	16.17	16.89	15.72	15.21	16.32	11.96
en**	(65.40)	(62.36)	(63.32)	(59.34)	(62.08)	(61.64)	(59.35)	(62.97)
ol	—	—	2.60	1.98	0.81	3.35	—	—
fo*** ...	—	—	(61.04)	(56.98)	(59.77)	(59.32)	—	—
mt	2.28	13.45	12.34	10.90	9.41	12.96	9.47	3.38
ap	0.05	—	—	—	—	—	—	0.21
il	0.61	3.99	3.67	3.46	2.72	4.44	3.10	0.95
Total	99.58	100.21	100.15	100.59	98.79	101.11	99.24	100.33
CI	53.65	49.48	51.03	49.59	52.19	49.35	50.74	49.75

Modes (vol. %)

Ol	—	—	—	—	—	—	—	—
Opx	—	—	—	—	—	—	—	—
Cpx	—	49.3	38.7	40.9	45.8	36.6	41.5	5.5
Pl	80.5	46.9	50.3	46.8	50.5	40.9	53.2	84.5
Bi	—	—	—	—	—	—	—	—
Q	10.0	—	—	—	—	—	—	6.5
Fe-Ti-Ox	—	3.7	10.9	12.3	3.7	22.4	5.0	—
Others ...	9.5	0.1	0.1	—	—	0.1	0.3	3.5
	100.0	100.0	100.0	100.0	100.0	100.0	100.0	100.0

CHEMISTRY OF THE SYÖTE SECTION

Chemical compositions for the Syöte section are presented in Tables 9—11. The chief emphasis in the analysis of the minor elements was placed upon those which form ores within basic magmas, namely Cr, V, Ni, Cu, Co and S, and including in addition Zn and Sr. Analyses of the minerals contained in the various rock types are given in connection with the description of these minerals, in Tables 2—8. The variations in the chemical components of the rocks and minerals discussed are plotted against structural height in Figures 12—14.

Among the trends in the chemical composition of the rocks (Figs. 12 and 13), SiO_2, Al_2O_3, CaO, Na_2O, K_2O and Sr form a group with a broadly similar variation, diminishing in amount with height in the marginal series and then reverting to a rising trend in the layered series proper. A marked fluctuation and scatter in the value is to be seen in the lower zone in particular, but a more even pattern prevails in the middle zone, while a general drop to a reduced level is to be found in the magnetite gabbro horizon in the upper zone.

A second group with broadly similar patterns of variation consists of MgO, Fe_2O_3, FeO, Cr and Ni, the concentration curves for which are roughly speaking a mirror image of those for the former group. Ni in particular, and also Cr, follow closely the trend in Mg, so that those rocks rich in Mg show extremely high Ni

Table 11.

Minor elements (ppm) in the Syöte layered series. (For sample classifications, see Table 1.

	1	2	3	4	5	6	7	8	9	10	11	12
Co	100	100	90	90	30	100	110	60	110	50	40	50
Cr	230	100	280	200	50	420	300	120	320	90	80	60
Cu	80	70	90	30	70	80	110	60	60	110	120	140
Ni	700	660	540	790	170	610	770	350	900	130	100	120
S	600	800	100	300	10	400	200	300	200	100	n.d.	200
Sr	200	300	200	300	500	200	200	400	200	300	500	300
V	100	100	100	100	100	100	100	100	100	100	200	200
Zn	80	100	80	120	40	90	90	60	100	70	50	60

Table 11. Continued

	13	14	15	16	17	18	19	20	21	22	23	24	25
Co	50	40	50	50	60	20	90	90	100	80	110	90	30
Cr	80	50	100	230	n.d.	140	n.d.	n.d.	n.d.	n.d.	40	30	70
Cu	80	90	80	100	200	n.d.	340	290	540	350	450	520	n.d.
Ni	100	100	120	130	90	30	170	150	150	130	140	130	50
S	—	100	100	100	200	100	200	200	300	100	800	1 800	100
Sr	300	300	300	300	300	600	200	200	200	200	200	200	500
V	200	200	200	200	200	100	2 200	1 900	1 900	1 600	2 100	1 500	100
Zn	80	60	80	80	70	20	90	90	100	100	100	90	60

n.d. = not detected.

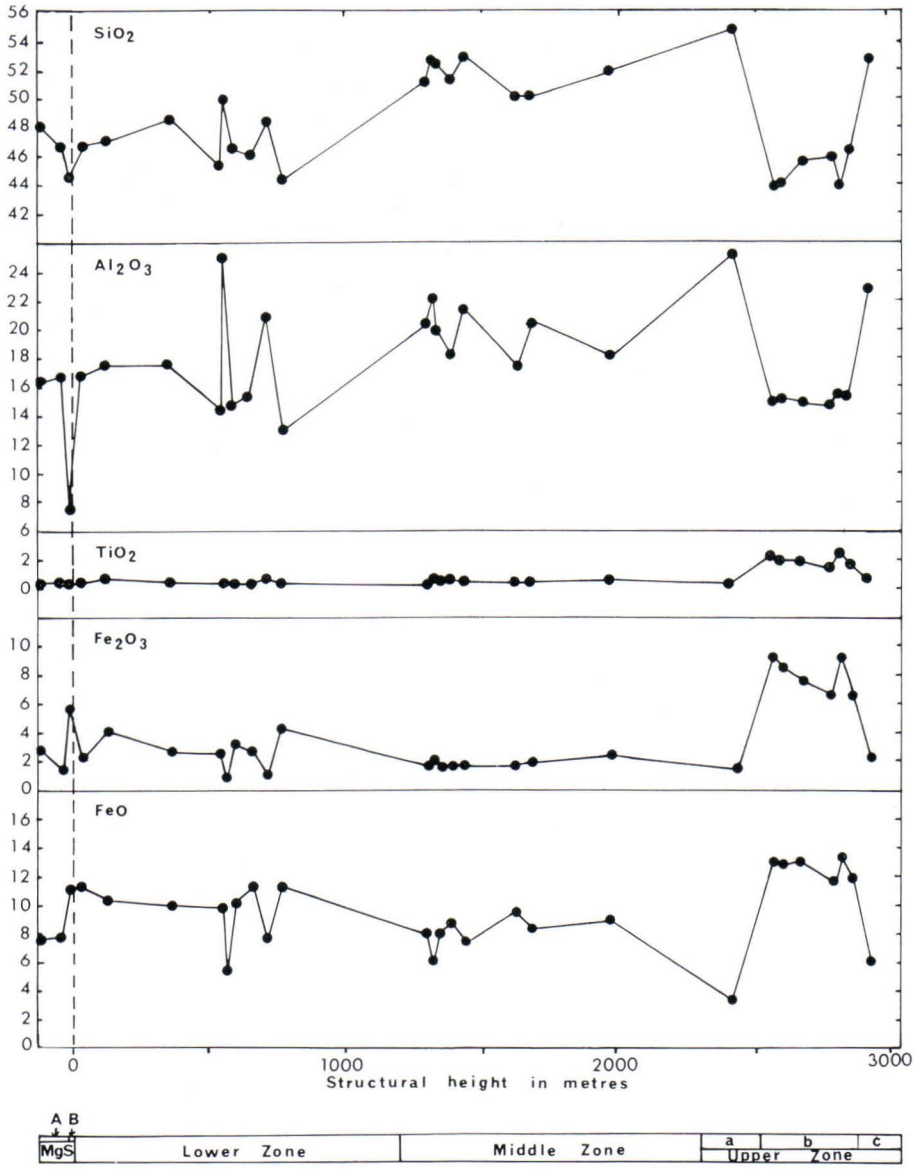

Fig. 12. Variations in the amounts of major components plotted against structural height.

concentrations, over 900 ppm in places in the layered series, and as high as over 3000 ppm in the marginal series. In contrast, the actual amounts of Cr present are relatively low, seldom exceeding 400 ppm in the same horizons. The low concentrations of TiO_2 are particularly surprising, its proportions lying well below 0.5 %

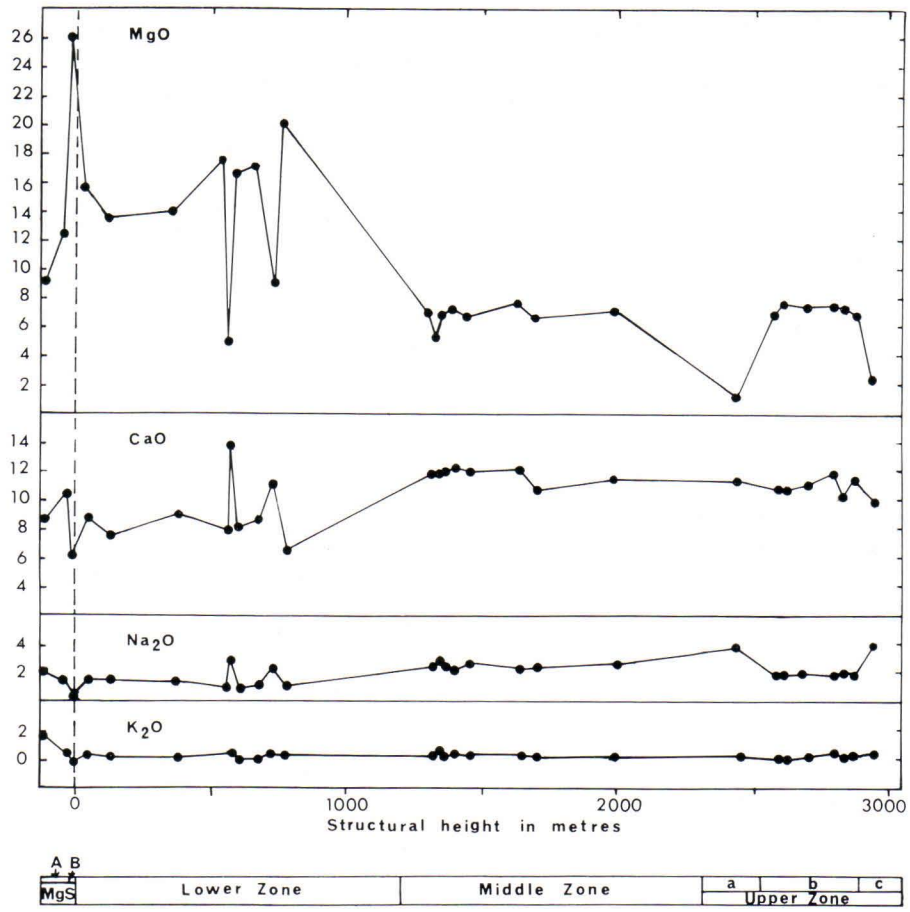

Fig. 12. Contd.

in the rocks of the lower zone, reaching a minimum of 0.15 %, and only rising to the 0.5 % in a few places in the middle zone. The highest TiO_2 concentrations are recorded in the upper zone magnetite gabbro horizon, and even here they do not exceed by very much the normal TiO_2 concentrations of rocks of a gabbro composition. Vanadium content tends to vary in a similar manner to FeO, Fe_2O_3 and TiO_2, being low in the lower and middle zones, but high in the magnetite gabbro horizon of the upper zone, and Cu similarly achieves very much higher concentrations in this latter horizon. The concentrations of Co, Zn and S show parallel trends in the lower and middle zones. The lower part of the lower zone shows a relatively high concentration of S, around 600—800 ppm, but this then falls in the upper part to a minimum of 10 ppm. The S concentration also increases in the magnetite gabbro horizon.

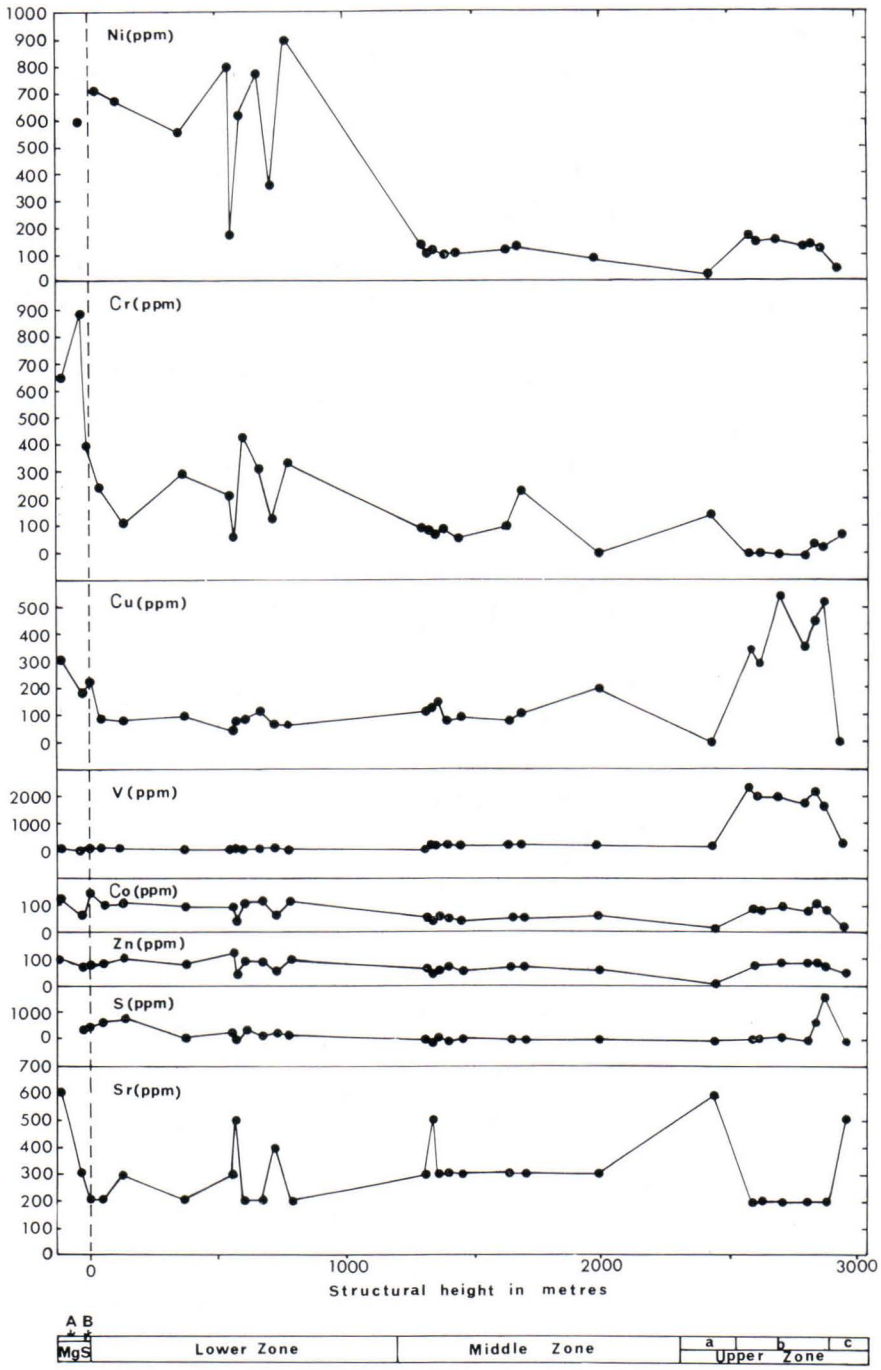

Fig. 13. Variations in the amounts of minor elements plotted against structural height.

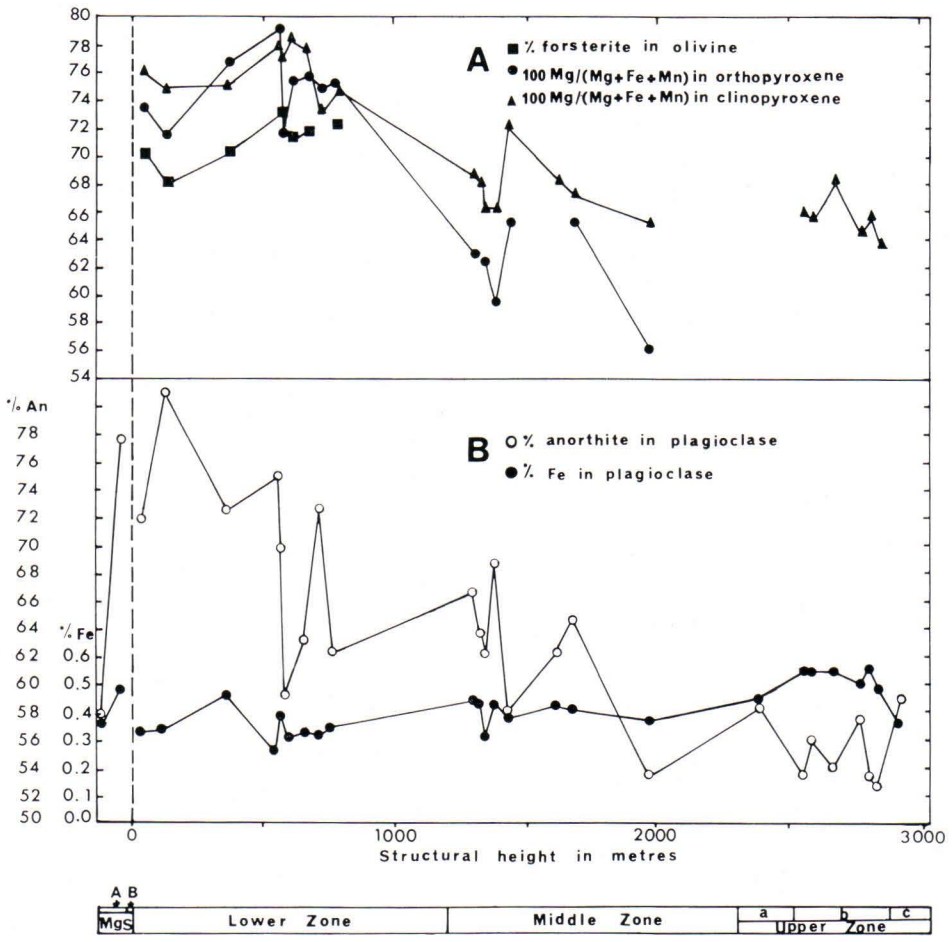

Fig. 14. Variations in the mineral compositions plotted against height in the sequence. (Fe in weight %, others in mol.%)

As one might expect, the general trend in the chemical composition of the minerals (Fig. 14) is broadly speaking for a decrease in Mg content in the ferromagnesian silicates and a decrease in An content in the plagioclase, although there is a certain amount of variation and oscillation to be observed in the curves concerned. Similar variations in Mg content are recorded in the cases of olivine, orthopyroxene and clinopyroxene, whereas the changes in An content in the plagioclase are quite astonishing in comparison with those observed in the Mg-Fe silicates, being parallel in some instances and directly opposed in others. It may also be noted that the plagioclase contains a small amount of Fe, varying between 0.26 % and 0.56 %. It seems, in fact, that the Fe concentration in plagioclase varies in an inverse manner to that of An, as has been mentioned above (see p. 22).

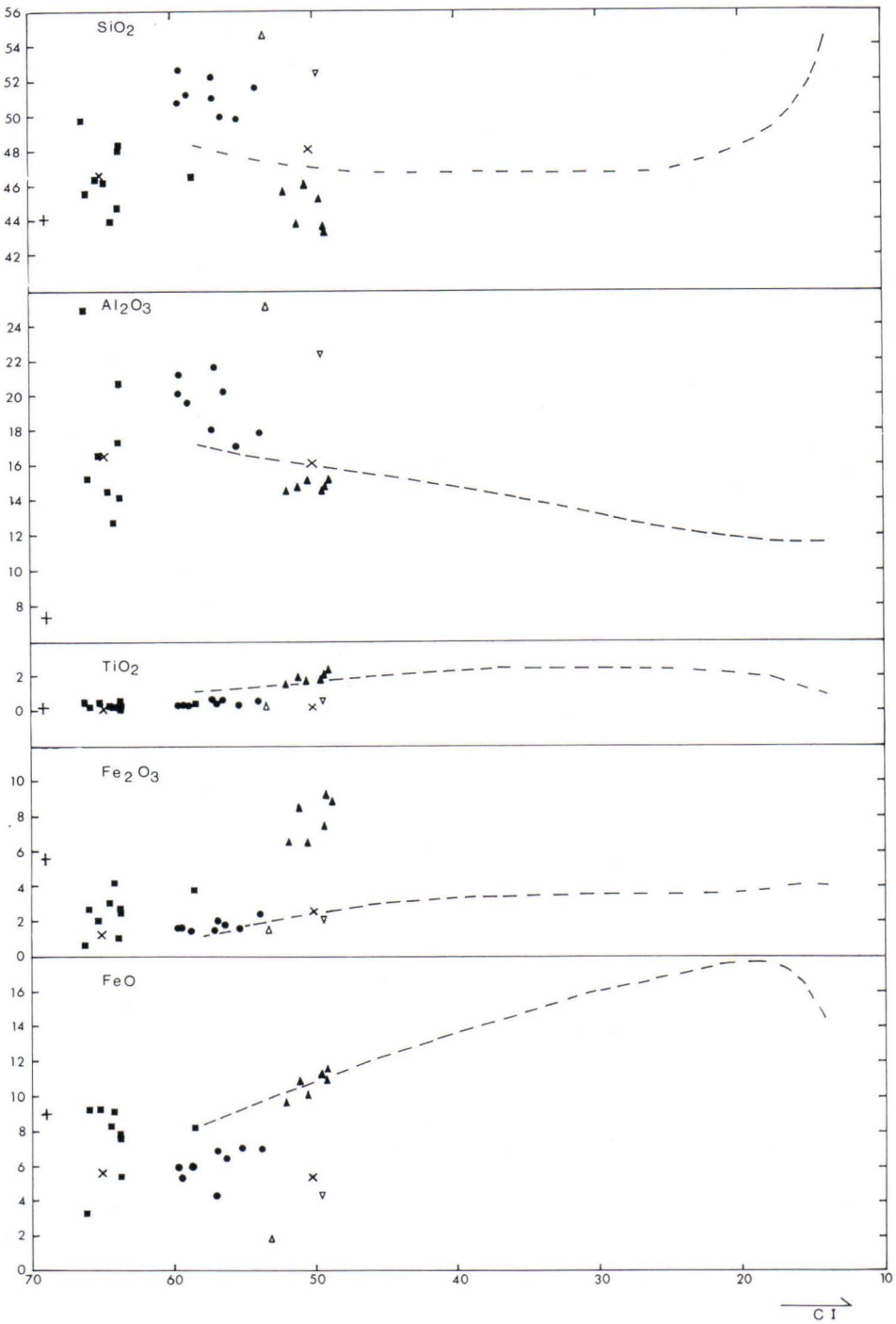

Fig. 15. Variations in the amounts of major components plotted against the crystallization index. The differentiation trend for the Skaergaard partial magma is shown for comparison purposes.

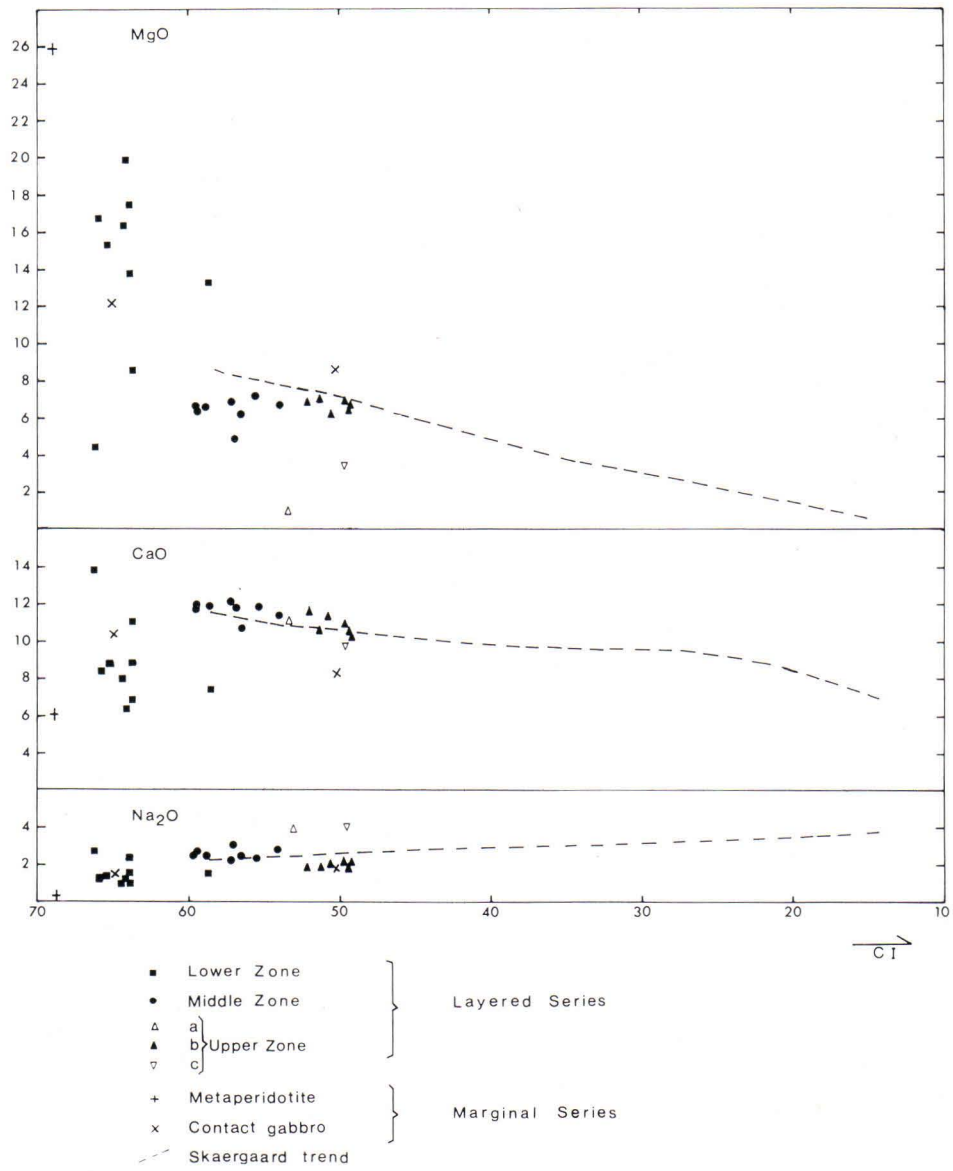

Fig. 15. Contd.

The chemical analyses (Tables 9 and 10) were also used to calculate normative mineral compositions for the rocks and the Crystallization Index of Poldervaart & Parker (1964). The relationship between this index and the chemical components is depicted for the major components in Fig. 15 and for the minor elements in Fig. 16. For comparison purposes, the differentiation trends of the Skaergaard partial

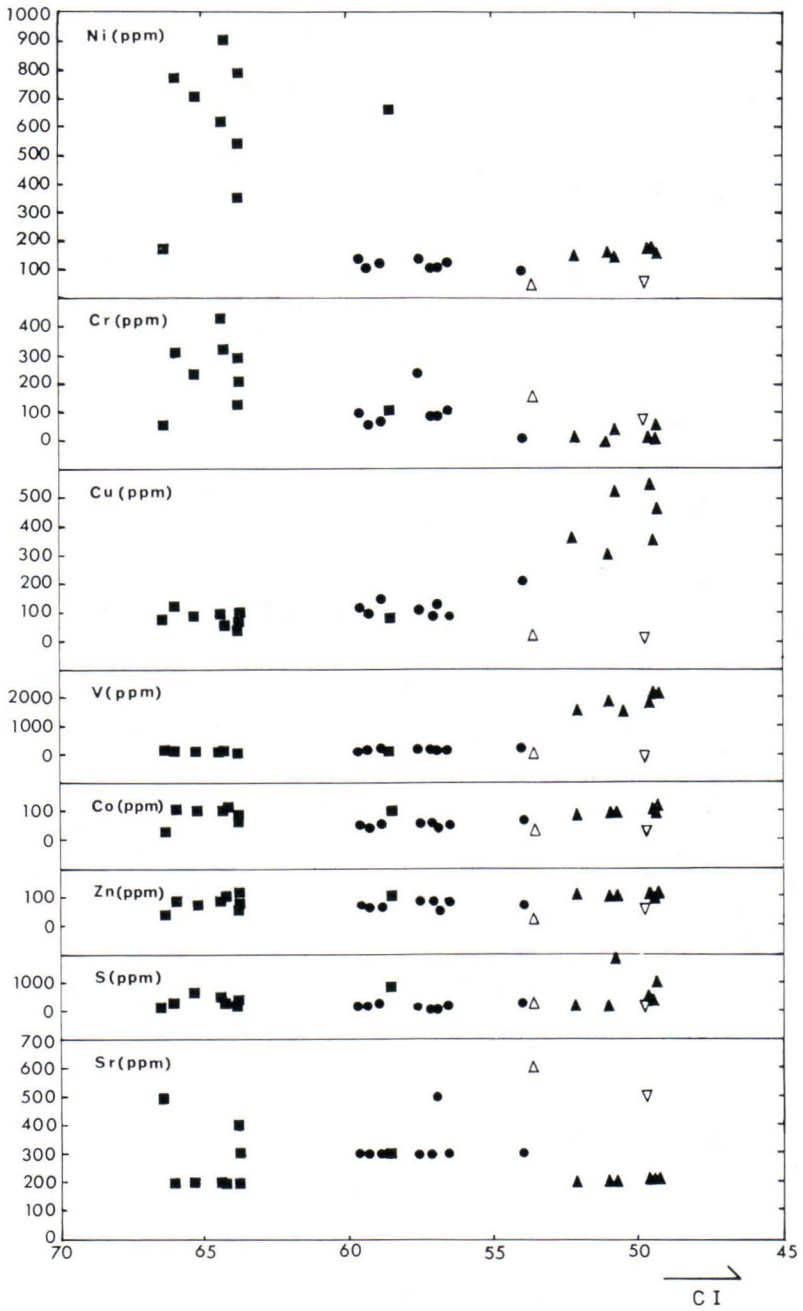

Fig. 16. Variations in the amounts of minor elements in the layered series plotted against the crystallization index. For key to symbols, see Fig. 15.

magma (Poldervaart & Parker 1964) is superimposed upon the former figure for each of the components studied. The outstanding features here are the pronounced scatter of the results and the shortness of the differentiation trends compared with those for Skaergaard.

The extremely marked scatter found in the patterns depicting the chemical composition of the rock types versus structural hight (Figs. 12 and 13) may be explained by the fact that not all the samples represent 'average rocks' (Wager 1960), for some are included which represent leucocratic and melanocratic horizons. At the same time oscillations are to be found in the composition curves (Figs. 15 and 16), while changes occur in the composition of the Mg-Fe silicates and plagioclase (Fig. 14), all of which would suggest that the crystallization of the section as a whole was an extremely complex sequence of events.

ESTIMATIONS OF CRYSTALLIZATION TEMPERATURE

Equilibration temperatures for orthopyroxene—augite pairs calculated according to the method of Wood & Banno (1973) are presented in Table 12, and selected temperatures are indicated in Fig. 17. These calculations are hampered to some extent by the recrystallization in the subsolidus state, which is difficult to take into account in microanalysis. It is probable that the most accurate temperature estimate for the lower zone is that given by sample no. 7, approx. 1 000°C. The inverted

Table 12.

Calculated equilibration temperatures for clinopyroxene — orthopyroxene pairs in the Syöte layered series, method after Wood & Banno (1973).

Sample	Temperature (°C)
1	922
2	930
3	992
4	974
5	920
6	948
7	1 003
8	964
9	919
10	944
10	964[1])
12	896
13	895
14	894
16	921
17	867

[1]) Calculated using the estimated composition of the original pigeonite (see Table 4.)

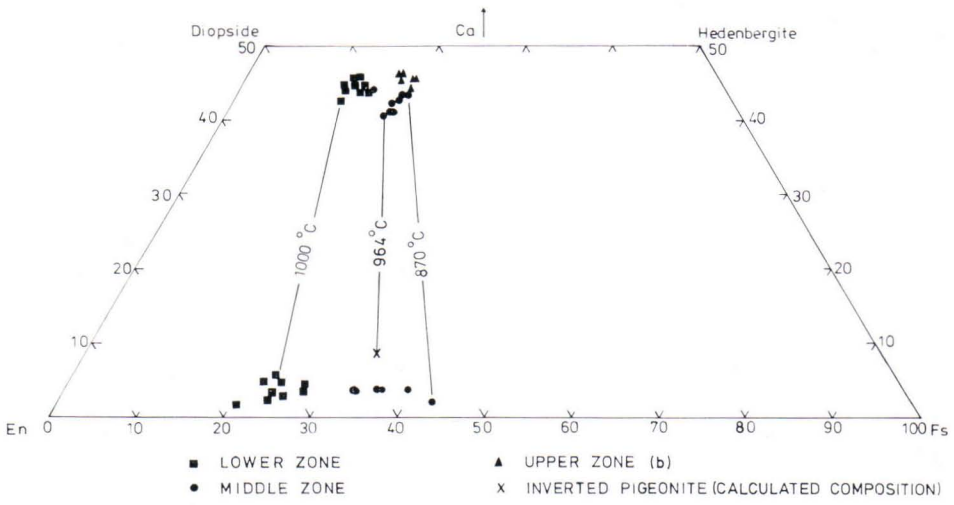

Fig. 17. Crystallization trend for pyroxene in the Syöte layered series, and selected equilibration temperatures for pyroxenes, calculated according to Wood & Banno (1973).

pigeonite of the lowermost horizon of the middle zone, the original composition of which is detailed in Table 4, represents fairly accurately the point at which orthopyroxene ceases to crystallize and its place is taken by pigeonite. Using the method of Wood & Banno, a equilibration temperature of 964°C is obtained for this pigeonite together with the augite which crystallized simultaneously. A corresponding pyroxene pair from Bushveld is reported to have given a result of 1005°C (Wood & Banno 1973). According to Brown (1957, Fig. 5) a pigeonite of this kind would crystallize at approx. 1070°C.

An attempt was also made to determine the crystallization conditions from magnetite—ilmenite pairs employing the T-f(02)-X relations of Buddington & Lindsley (1964). The resulting figures for temperature and oxygen fugacity are presented in Table 7, one determination in which is based on discrete titaniferous magnetite and ferrian ilmenite, while the others rely on either combined ilmenomagnetite-ilmenite grains or a titaniferous magnetite matrix with ilmenite lamellae. This method based on the magnetite—ilmenite pair nevertheless presupposes the crystallization of iron-titanium oxides in equilibrium one with another and the preservation of their original composition. The iron-titanium oxides of the samples studied here, however, regularly contain evidence of subsolidus recrystallization, and thus their composition cannot be used for the direct determination of their primary magmatic crystallization conditions (cf. Buddington & Lindsley 1964, Mathison 1975, Himmelberg & Ford 1977).

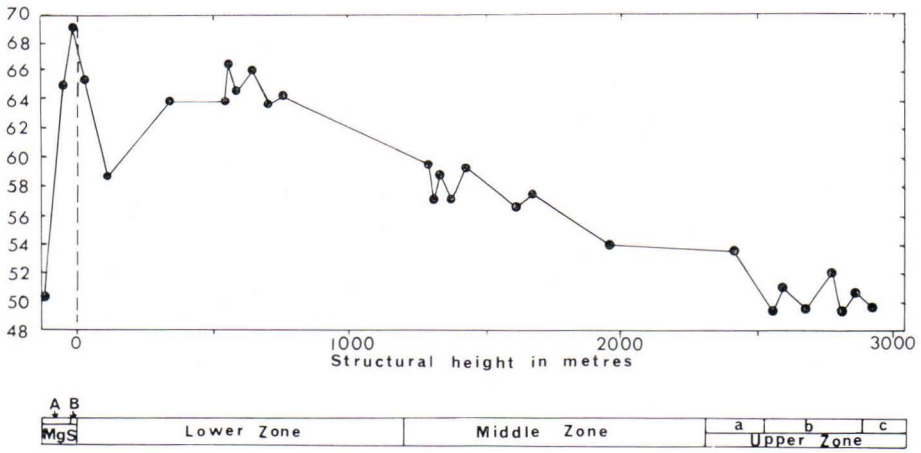

Fig. 18. Plot of the crystallization index of rocks from the Syöte marginal and layered series versus structural height.

ON THE PETROGENESIS OF THE SYÖTE SECTION

Since no 'chilled margin' has been found in the Syöte section, no direct evidence is available on the composition of its parental magma. On the other hand, the relatively small variation in the chemical compositions of the rock types (Tables 9 and 10) offer some basis for a rough estimate of the nature of this magma. Since the dominant rocks are various norites and gabbros rich in plagioclase, which correspond in their composition to the Al_2O_3-rich tholeiites and olivine tholeiites in the basalt classification of Yoder & Tilley (1962), the composition of the parental magma may be set somewhere between the values for these two. A high Al_2O_3 content may be regarded as being due to an accumulation of ferromagnesian silicates as the magma was ascending. The chemical composition of the rock types is also characterized by a high MgO content and low TiO_2, which would argue in favour of high magnesium basaltic or komatiitic parental magma.

The marginal series represents a zone of crystallization which formed at the early stages in the formation of the magma chamber, showing 'reversed' fractionation (Figs. 12—15 and 18) similar to that found in the Muskox and Jimberlana layered intrusions (McClay & Campbell 1976). The crystallization of the marginal series is associated with a separation of immiscible Ni-Cu-Fe sulphide liquid from the silicate melt as a consequence of which a weak sulphide dissemination is to be found in the series (cf. Piirainen *et al.* 1977).

The present layered series includes alternating melanocratic and leucocratic layers and well-developed igneous lamination, especially in its lower parts, structural features which may be explained on the basis of gravitative differentiation and

convection currents. The variation diagrams depicting the advance of the crystallization process (Figs. 14 and 18) nevertheless contain interruptions which cannot be explained by a simple crystallization model. This is presumably a case of 'macro-rhythmic layering', a feature whose origins have been interpreted in three different ways:

1. According to Jackson (1961), crystallization occurs from a stagnant zone of magma below the intersection of the curves of the adiabatic temperature gradient and the meltingpoint gradient, and continues until the heat released by crystallization raises the temperature of the stagnant layer to the melting-point temperature gradient. The zone of crystallization is now at a super-adiabatic temperature, and is in a favourable condition to join the convection of the main body of magma.

2. According to Wager & Brown (1968), the type of macrolayering found in the Rhum and Bushveld intrusions may result from the order of nucleation of the cumulus phases from a super-cooled magma.

3. The formation of macro-rhythmic units is due to periodic influxes of undifferentiated magma. Each influx mixes with the fractioned magma in the chamber, making it more ultrabasic and raising its temperature, resulting in a repetition of the mineral assemblage (Irvine & Smith 1967).

The last of these explanations would apply best in the present case, and would also assist our understanding of why the total differentiation remained so small even though the section is some 3 km thick. Not only would new magma have entered the chamber from time to time during the crystallization process, but also the crystallization conditions in the magma chamber could have been transformed by the eruption of magma to form overlying surface volcanoes.

As the lower zone of the layered series crystallized, olivine, bronzite and plagioclase occurred as cumulus minerals. At the boundary between the lower and middle zones the crystallization of olivine then came to an end, and instead of bronzite, pigeonite began to be formed, and Ca-rich clinopyroxene, which occurs in the lower zone only as an intercumulus mineral began to crystallize as a cumulus mineral. The levelling out of the fluctuations in the diagrams depicting the crystallization indices and compositions of minerals in the middle zone is an indication that by this stage the magma chamber had reached its full proportions and crystallization was now taking place within a closed system. As crystallization advanced within this same closed system the water content of the magma increased and at the same time its density decreased, the outcome of which was a pronounced accumulation of plagioclase downwards to form subzone a of the upper zone. Meanwhile the increase in oxygen fugacity led to the crystallization of ilmenomagnetite, and thus to the creation of the magnetite gabbro horizon, in which the primary minerals are plagioclase, ilmenomagnetite, clinopyroxene and probably pigeonite.

Horizon c of the upper zone, which overlies the magnetite gabbro and is composed of leucogabbro and anorthosite, contains a plagioclase with an An content of less than 60 %, so that this cannot be a downward-growing upper cumulate, but rather

a crystallization from the residual magma, and must be younger than the magnetite gabbro horizon. This residual magma contained high proportions of SiO_2, Al_2O_3, and CaO and a certain amount of Na_2O, FeO, Fe_2O_3 and MgO.

ACKNOWLEDGEMENTS

The authors wish particularly to thank the Institute of Electron Optics of the University of Oulu for valuable co-operation with the mineral analyses, and Rautaruukki Co. for the whole-rock analyses. The manuscript was translated into English by Mr. Malcom Hicks, M.A. and to him we wish to express our gratitude. We would also like to thank Dr. Atso Vorma for critically reading the final text and providing valuable suggestions. Professor Herman Stigzelius, Director of the Geological Survey of Finland, kindly arranged for the publication in the Survey's Bulletin series. This investigation was supported by the IGCP Project 74/1/91, »Metallogeny of the Precambrian» and this support is gratefully acknowledged.

REFERENCES

Alapieti, T., Hugg, R., Piirainen, T. & Ruotsalainen, A. (1979). The ultramafic and mafic intrusion at Näränkävaara, northeastern Finland. Geol. Surv. Finland, Rep. Invest. No. 35. 31 p.

Brown, G. M. (1957) Pyroxenes from the early and middle stages of fractionation of the Skaergaard intrusion, East Greenland. Miner. Mag. 31, 511—343.

Buddington, A. F. & Lindsley, D. H. (1964) Iron-titanium oxide minerals and synthetic equivalents. J. Petrology 5, 310—357.

Carmichael, I. S. E. (1967) The iron-titanium oxides of salic volcanic rocks and their associated ferromagnesian silicates. Contr. Mineral. and Petrol. 14, 36—64.

Enkovaara, A., Härme, M. & Väyrynen, H. (1953) Kivilajikartan selitys C 5—B 5, Oulu—Tornio. English summary: Explanation to the map of rocks. General Geological Map of Finland, 1:400 000. 153 p.

Frick, C. (1973) Intergrowths of orthopyroxene and ilmenite from Frank Smith Mine, near Barkly West, South Africa. Trans. geol. Soc. S. Afr. 76 (3), 195—200.

Haselton, J. D. & Nash, W. P. (1975) Ilmenite-orthopyroxene intergrowths from the moon and Skaergaard intrusion. Earth Planet. Sci. Lett. 26, 287—291.

Himmelberg, G. R. & Ford, A. B. (1977) Iron-titanium oxides of the Dufek intrusion, Antarctica. Am. Miner. 62, 623—633.

Irvine, T. N. & Smith, C. H. (1967) The ultramafic rocks of the Muskox Intrusion, Northwest Territories, Canada. Pp. 38—49 *in* Ultramafic and related rocks, ed. by P. J. Wyllie. New York, John Wiley and Sons.

Jackson, E. D. (1961) Primary textures and mineral associations in the ultramafic zone of the Stillwater Complex, Montana. U.S. Geol. Surv. Prof. Paper 358, 1—106.

Juopperi, A. (1977) The magnetite gabbro and related Mustavaara vanadium ore deposit in Porttivaara layered intrusion, north-eastern Finland. Geol. Surv. Finland, Bull. 288. 68 p.

McClay, K. & Campbell, I. H. (1976) The structure and shape of the Jimberlana Intrusion, Western Australia as indicated by a combined geological and geophysical investigation of the Bronzite Complex. Geol. Mag. 113, 129—139.

Mäkelä, T. (1975) Emäksisen magman kiteytyminen ja differentiaatio Porttivaaran alueella, Koillismaalla. Master's thesis. Manuscript at the Department of Geology, University of Oulu, Finland. 103 p.

Mason, P. K., Frost, M. T. & Reed, S. J. B. (1969) B.M.-I.C.-N.P.L. computer programs for calculating corrections in quantitative x-ray microanalysis. Nat. Phys. Lab. IMS Report 2.

Mathison, C. I. (1975) Magnetites and ilmenites in the Somerset Dam layered basic intrusion, southeastern Queensland. Lithos 8, 93—111.

Piirainen, T., Alapieti, T., Hugg, R. & Kerkkonen, O. (1977) The marginal border group of the Porttivaara layered intrusion and related sulphide mineralization. Bull. Geol. Soc. Finland 49 (2), 125—142.

Piirainen, T. Hugg, R., Aario, R., Forsström, L., Ruotsalainen, A. & Koivumaa, S. (1978) Koillismaan malmikriittisten alueiden loppuraportti. English summary: The report of the Koillismaa Research Project. Geol. Surv. Finland, Rep. Invest. No. 18. 51 p.

Piirainen, T. & Juopperi, A. (1968) Die Titaneisenerzlagerstätte von Porttivaara und ihre Entstehung. Nordia 1968, 5. 24 p.

Poldervaart, A. & Parker, A. B. (1964) The crystallization index as a parameter of igneous differentiation in binary variation diagrams. Am. J. Sci. 262, 281—289.

Ruotsalainen, A. (1977) Koillismaan intruusioiden rakenteen geofysikaalisesta tulkinnasta. Master's thesis. Manuscript at the Department of Geophysics, University of Oulu, Finland. 64 p.

Väyrynen, H. (1954) Suomen kallioperä, sen synty ja geologinen kehitys. Helsinki, Otava. 260 p.

Wager, L. R. (1960) The major element variation of the Layered Series of the Skaergaard Intrusion and re-estimation of the average composition of the Hidden Layered Series and successive residual magmas. J. Petrology 1, 364—398.

Wager, L. R. & Brown, G. M. (1968) Layered igneous rocks. Edinburgh: Oliver and Boyd. 588 p.

Wood, B. J. & Banno, S. (1973) Garnet-orthopyroxene and orthopyroxene-clinopyroxene relationships in simple and complex systems. Contr. Miner. and Petrol. 42, 109—124.

Yoder, H. S., Jr. & Tilley, E. (1962) Origin of basalt magmas: An experimental study of natural and synthetic rock systems. J. Petrology 3, 342—532.

ISBN 951-690-100-x
ISSN 0367-522x